Interreg Euro-MED

Co-funded by the European Union

FRED

Title of document:

Data collection and processing methodology for wildfire prevention and mitigation

Work package 1

Defining and implementing tools for wildfire prevention and mitigation

Activity 1.1

Implementation methodology

Output 1.1

Data collection and processing methodology for wildfire prevention and mitigation

Project full title:	Fire free MED
Mission:	Protecting, restoring and valorising the natural environment and heritage – Natural heritage
Priority:	Greener MED
Specific objective:	RSO 2.4 Promoting climate change adaptation and disaster risk prevention, resilience, taking into account eco-system-based approaches

Partner in charge: University of Rijeka, Faculty of Maritime Studies

Partners involved: University of Rijeka, Faculty of Maritime Studies, Democritus University of Thrace, Fire rescue service Sežana, Rocca di Cerere UNESCO Global Geopark, The Municipality of Ulcinj, RGO Communications Ltd., The National Park UNA, Public fire brigade of the Town of Mali Lošinj, Centre of Integrated Geomorphology for the Mediterranean Area, CIMBAL – Intermunicipal Community of Baixo Alentejo

Status: Final

Distribution: Public

Date of production: 16.12.2024

Revision chart and history log

Author in charge	Status	Date of production
Name Surname	draft/final/N version	DD.MM.YYYY
Tomislav Krljan	draft	18.11.2024
David Brčić	draft	06.12.2024
Pantelis Xofis	draft	10.12.2024
Damir Obad	draft	13.12.2024
Neven Grubišić	Final	16.12.2024

Table of Contents

1. Introduction 7
2. Methodological approaches 8
2.1. Land uses 9
2.2. Spatial data 9
2.3. Aspect 9
2.4. Slope 10
2.5. Geomorphology 10
2.6. Canopy Height 11
2.7. Tree cover density 11
2.8. Roads and buildings network 12
2.9. NDVI 12
2.10. Sentinel 2 images 14
2.11. Planet image 16
3. Fuel Mapping Methodological Approach 18
4. Fire Risk Assessment Methodological Approach 21
5. Weather forecast data 24
5.1. How to download the MISTRAL forecast data using the APIs 26
5.2. Meteorological variables of interest 27
5.3. How to retrieve the FWI input parameters from MISTRAL data 27
6. UAS application for data collection 33
6.1. Payloads 33
6.1.1. Visual RGB camera 33
6.1.2. Thermal camera 34
6.1.3. Light Detection and Ranging sensor, LiDAR 35
6.1.4. Multispectral camera 37
6.1.5. Loudspeaker 39
6.1.6. Spotlight 39
6.1.7. Real-Time Kinematic module 39
6.1.8. Parachute 40
6.1.9. Software Development Kit 40
6.1.10. Postprocessing data analysis software 42
6.2. Data collection techniques 42

6.2.1. 2D/3D Photogrammetry 43
6.2.2. Ortho-mosaic Mapping 44
6.2.3. LiDAR 44
6.2.4. Multispectral and hyperspectral imaging 45
6.2.5. Thermal Imaging 47
6.2.6. Real-time data transfer and live video streaming 48
6.2.7. Geometrical evaluation 49
6.2.8. Aerial Action 49
6.2.9. Sound diffusion technique 49
6.2.10. Lighting technique 51
6.3. Mapping approaches 54
6.3.1. Rectangle mapping 54
6.3.2. Spiral mapping 54
6.4. Interoperability 55
6.5. Scope of application/Mission actions/mode of operation: 59
6.5.1. General considerations and an overview in data collection techniques' applications 59
6.5.2. Mission actions' application examples 60
6.5.3. Operational capacity of the FRED platform – data transmission and viewing optimisation 62
7. Concluding remarks 64
Appendix A: 65
Appendix B: 67
References 69

List of Figures

Figure 1. Map that showcases the location of the different pilot areas across Europe. 8
Figure 2. Fire Risk Assessment – Estimation of fire behaviors parameters 17
Figure 3. OBIA Classification Algorithm. 19
Figure 4. COSMO-5M: Forecasted Air temperature (°C) at noon on 12 July, 2024. 25
Figure 5. COSMO-2I: Air temperature and Relative humidity forecasted at noon on 22 June, 2024. 31
Figure 6. COSMO-2I: 24-h precipitation and Wind speed at noon on 22 June, 2024. 32
Figure 7. (a) DJI Zenmuse H30; (b) DJI Zenmuse H20; (c) DJI Zenmuse P1; Source: DJI webpage 34
Figure 8. (a) DJI Zenmuse H30T; (b) DJI Zenmuse H20T; (c) DJI Zenmuse XT V2; Source: DJI Webpage 35
Figure 9. LiDAR principle. Source: DJI site 36
Figure 10. (a) DJI Zenmuse L2; (b) DJI Zenmuse L1; Source: DJI Webpage 37
Figure 11. DJI Zenmuse X3. Source: DJI Webpage 38
Figure 12. UAS data acquisition and processing: A general workflow (10.1007/s12518-013-0120-x) 43
Figure 13. Different modes of imaging illustrating the benefits of hyperspectral imaging. (https://www.middletonspectral.com/resources/what-is-hyperspectral-imaging/) 46
Figure 14. The fire event viewed with two different cameras, conventional RGB (right) and infrared (left); Source: (https://extension.okstate.edu/fact-sheets/using-drones-with-infrared-capabilities-to-monitor-fire-behavior.html) 49
Figure 15. UAS rectangle mapping data collection technique. 54
Figure 16. UAS spiral path (source: https://doi.org/10.5755/j01.itc.45.1.12413) 55
Figure 17. UAS spiral technique. 55
Figure 18. UAS aerial surveying and mapping techniques, and levels of interoperability 57
Figure 19. UAS aerial surveying and mapping techniques, and levels of interoperability (10.3390/drones6060147). 60
Figure 20. Drone support for Search and Rescue Operations (https://altigator.com/en/drones-for-search-rescue-missions/) 61

List of Tables

Table 1. Spectral and Spatial characteristics of Sentinel 2 images. 15
Table 2. Spectral and Spatial characteristics of Planet images. 16
Table 3. Compatibility of payloads with the UAS system. 41
Table 4. UAS sound diffusion geographical features. 50
Table 5. UAS lighting geographical and effective features. 51
Table 6. UAS aerial action lighting technique: key features 52
Table 7. Interoperability matrix. 56
Table 8. Description and interoperability between data collection techniques. 57
Table 9. Examples of particular UAS data collection techniques' applications 59
Table 10. Steps in Hot Spot Detection with Multiple Techniques. 61

List of abbreviations and terms

Abbreviation	Definition
API	Application Programming Interface
CDO	Climate Data Operators
CHM	Canopy Height Models
CORINE	Coordination of Information on the Environment
COSMO	Consortium for Small-scale Modeling
CS	Coordinate System
DEM	Digital Elevation Model
DTM	Digital Terrain Model
EEA	European Environment Agency
ECMWF	European Centre for Medium-Range Weather Forecasts
EFFIS	European Forest Fire Information System
FARSITE	Fire Area Simulator - model development and evaluation
FRED	Fire Free MED
FDI	Fire Danger Index
FI	Fire Intensity
FWI	Fire Weather Index
GDAL	Geospatial Data Abstraction Library
GIS	Geographical Information System
GRIB	General Regularly distributed Information in Binary form
HI	Human Index
MISTRAL	Meteo Italian Supercomputing Portal
NDVI	Normalized Difference Vegetation Index
NetCDF	NETwork Common Data Form
OBIA	Object-Based Image Analysis
PH	Pyric History Index
ROS	Rate of Spread

TIN	Triangulated Irregular Network
UAS	Unmanned Aircraft System
UTC	Coordinated Universal Time
WKT	Well-Known Text
WMO	World Meteorological Organisation
WSL	Windows Subsystem for Linux

1. Introduction

Wildfires pose an increasingly severe threat across the Mediterranean region, driven by the growing impacts of climate change and intensified human activity. Addressing this challenge requires a harmonized, cross-border approach that integrates advanced technologies with established practices. The FRED project aims to meet this need by deploying state-of-the-art ICT and UAS (Unmanned Aircraft Systems) solutions to support climate adaptation and disaster risk management—specifically focusing on wildfire prevention and mitigation.

This document outlines the shared methodology developed by project partners from seven Mediterranean countries, which provides a common framework for data collection, processing and operational deployment. The methodology supports the development and implementation of practical tools that can be scaled and transferred across national borders, enhancing the region's collective capacity to anticipate, respond to and mitigate wildfire events by supporting operational capacity in wildfire suppression.

Drawing from the experience and outcomes of past initiatives, the paper consolidates lessons learned and technical knowledge to inform pilot activities in six targeted areas—Kras karst in Slovenia, Rocca di Cerere UNESCO Geopark in Sicily, Una National Park in Bosnia and Herzegovina, Municipality of Ulcinj in Montenegro, Lošinj Island in Croatia and Baixo Alentejo region in Portugal. It defines a cohesive strategy encompassing the design and deployment of ICT / UAS tools, sensor integration, data handling workflows and site-specific operational planning. Each pilot scenario contributes to the overarching goal of building a more resilient and responsive wildfire management system.

This output provides a summary of methodological framework applied for data collection, processing and further utilization.

2. Methodological approaches

To ensure the project's objectives are met effectively, a robust and comprehensive methodological framework has been developed. This section outlines the various methods, tools, and spatial datasets that form the foundation of our analyses across the selected pilot areas. From the strategic selection of diverse Mediterranean regions to the integration of advanced geospatial data, land use analysis, and remote sensing technologies, each methodological component contributes to a thorough understanding of local landscapes, land cover dynamics, and wildfire risk factors. The following subsections describe these approaches in detail, highlighting how they work together to support informed decision-making and sustainable land management within the project.

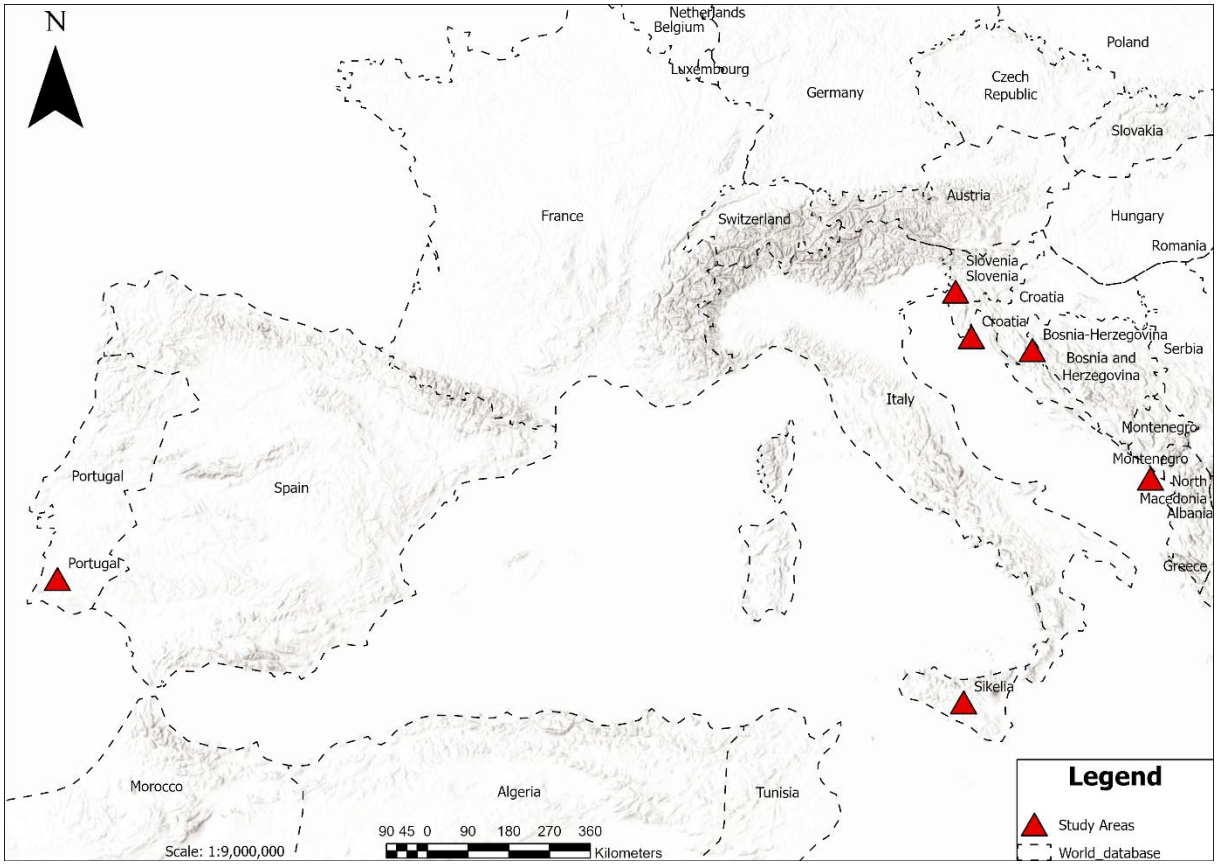

Figure 1. Map that showcases the location of the different pilot areas across Europe.

The project concentrates on six specific regions within the Mediterranean, serving as pilot areas for our initiatives. These regions encompass the following European countries: Croatia, Slovenia, Montenegro, Bosnia and Herzegovina, Italy, and Portugal. For each region a specific selection of areas named pilot areas is made, where the project will concentrate its efforts and attention (Figure 1. Map that showcases the location of the different pilot

areas across Europ). The selection of these areas is strategic, allowing for a diverse representation of the Mediterranean basin and facilitating comprehensive testing and analysis of our project's methodologies and objectives across different cultural and geographical landscapes.

2.1. Land uses

The different land uses of the area, occur by analyzing the CORINE (Coordination of Information on the Environment) Land Cover map. This map is a detailed inventory of land cover across Europe, developed by the European Environment Agency (EEA). It classifies and maps land cover into various categories such as forests, grasslands, wetlands, urban areas, and agricultural lands. The map provides comprehensive spatial data that illustrates the distribution and extent of different land cover types within a specific region or country. It is created using satellite imagery and other geographic data sources, allowing for consistent monitoring and comparison over time. The CORINE Land Cover map is widely used for environmental assessments, spatial planning, biodiversity monitoring, climate change studies, and policy-making. It serves as a valuable tool for understanding landscape dynamics, identifying land use changes, assessing habitat fragmentation, and supporting sustainable land management practices across Europe and beyond.

2.2. Spatial data

As already mentioned at the start of the paper, each pilot area will be also followed by a Geo-Database which will include spatial data regarding the area and that will aid further in the project. In this chapter, geospatial data maps will be introduced first, followed by remote sensing data maps. The geospatial data maps will encompass various types, including an aspect map, slope map, TIN map, Canopy Height Model (CHM) map, tree cover density map, a roads and buildings map and finally an NDVI map for all seasons. Subsequently, remote sensing data maps will be presented, featuring images from the Sentinel-2 satellite across all seasons. These maps illustrate the data that will be incorporated into Croatia's final Geo-Database, providing invaluable insights for the analysis of the region.

2.3. Aspect

An aspect map provides a detailed representation of a terrain (or any continuous surface) by illustrating the direction (aspect) of its slopes. In this type of map, aspect categories are represented by different colors such as red, orange, yellow, and so on. The degree of slope is conveyed through the

saturation or brilliance of these colors, where steeper slopes are depicted with brighter colors. This approach creates a visually informative map, with the colors displayed as shown on the right. By analyzing the colors, you can identify patterns in the landscape, such as predominant orientations of hillsides, valleys, and other landforms.

2.4. Slope

A slope map is a thematic map representing the steepness or incline of terrain, calculated from topographic or digital elevation data and expressed in degrees or percentage. It uses color gradients to show different steepness levels, with flatter areas in lighter colors and steeper areas in darker colors. Derived from digital elevation models (DEMs) or topographic maps, slope maps are essential for urban planning, construction, agriculture, environmental management, hydrology, and recreational planning. They help identify suitable areas for building, farming, and understanding erosion patterns, water flow, and runoff. Steeper slopes, shown in darker colors, are more prone to erosion and may require special management, while gentler slopes, in lighter colors, are more suitable for various land uses. Slope maps are created by collecting elevation data, calculating slope using GIS software, and visualizing the data with a color gradient to highlight different levels of steepness across the terrain. Slope maps together with aspect maps can be a great representation of the landscape in an area and can also be helpful into facing wildfires and predicting their spread.

2.5. Geomorphology

All of the geomorphology maps will be constructed through Triangulated Irregular Network (TIN) models. These models generate continuous surfaces, like terrain elevation or temperature gradients. This surface is depicted as a collection of facets created by linking data points at nodes to form adjacent triangles. TINs are usually displayed using color-shaded relief to illustrate elevation, with shaded relief simulating sunlight illuminating the earth's surface. Adding color enhances the visibility of ridges, valleys, and hillsides, showing their respective heights. Viewing data in this manner can help clarify the locations of other map features. Tin can be used to display any one of three surface characteristics: slope, aspect, and elevation on your map and you can simulate shaded relief. You can also display contour lines representing lines of elevation change.

2.6. Canopy Height

A canopy height model (CHM) map is a specialized type of map that represents the height of vegetation, particularly trees, above the ground surface. It is created by subtracting the ground elevation data (digital terrain model or DTM) from the top-of-canopy elevation data (digital surface model or DSM). This map visually depicts the vertical structure of vegetation, highlighting the height variations across different areas. A CHM is essential for ecological studies, forest management, and environmental monitoring, as it provides detailed information about the biomass, canopy density, and forest health. By showing the distribution and height of vegetation, CHM maps help in understanding habitat diversity, assessing carbon storage, and planning conservation strategies. A CHM is also really useful for studying wildfires. CHMs provide valuable spatial information about the vertical structure of vegetation, including tree heights and canopy density. This data is crucial for understanding how wildfires spread and behave in different types of forested landscapes. By integrating CHM data with fire behavior models, researchers and fire managers can better predict fire behavior, assess potential fire hazards, and plan effective fire management strategies such as prescribed burns or fuel reduction treatments. Therefore, CHMs play a significant role in enhancing the accuracy and effectiveness of wildfire management and mitigation efforts.

2.7. Tree cover density

A tree cover density map is a visual representation that shows the extent and density of tree canopies across a specific geographical area, typically derived from satellite imagery and remote sensing data. These maps use various techniques to classify and quantify the amount of vegetation cover present, ranging from sparse to dense forests. They are invaluable tools for environmental monitoring, allowing researchers and policymakers to track changes in forest cover over time, assess habitat quality and biodiversity, and understand the carbon storage capacity of forests. Moreover, they are important data that can be used in predicting different things about wildfires, for example how wildfires might spread across a landscape. Integrating tree cover density maps with fire behavior models allows for more accurate wildfire risk assessments and helps prioritize areas for fire prevention measures, such as fuel reduction treatments or prescribed burns. Therefore, tree cover density maps play a significant role in enhancing wildfire management strategies and improving overall preparedness for fire events.

2.8. Roads and buildings network

A roads and buildings map provides a comprehensive view of the infrastructure and urban layout within a specific area. It typically displays the network of roads, highways, streets, and pathways, detailing their connectivity and hierarchy. Additionally, such maps depict the distribution and types of buildings, including residential, commercial, industrial, and public structures. This information is crucial for urban planning, transportation management, and emergency services, as it helps identify access points, traffic flow patterns, and areas of congestion. A roads and buildings map also plays a pivotal role in the analysis and prediction of wildfires by providing critical spatial information about the built environment and infrastructure. Such maps help identify urban areas, residential neighborhoods, industrial zones, and commercial districts, which are crucial for assessing the potential impact of wildfires on populated areas. Understanding the layout of roads and highways allows fire management teams to plan evacuation routes and access points for firefighting equipment. Moreover, the distribution of buildings and their proximity to vegetation can indicate areas of higher fire risk or vulnerability. Integrating this information with wildfire spread models enables more accurate predictions of fire behavior and potential paths of fire spread. Additionally, the map aids in prioritizing areas for wildfire prevention strategies, such as creating firebreaks, implementing building codes, and conducting community outreach for fire preparedness. Overall, a roads and buildings map enhances the effectiveness of wildfire analysis, planning, and mitigation efforts by providing essential spatial context and infrastructure details.

2.9. NDVI

The NDVI (Normalized Difference Vegetation Index) is a numerical indicator derived from satellite imagery that measures the density and health of vegetation in a specific area. It calculates vegetation greenness by comparing the reflectance of near-infrared (NIR) and red bands. Higher NDVI values indicate denser, healthier vegetation, while lower values signify sparse vegetation or non-vegetated surfaces like bare soil or water bodies. For predicting and mitigating wildfires, NDVI serves several critical purposes. High NDVI values indicate areas with abundant, potentially flammable vegetation, which can help identify regions at greater risk of wildfires. Conversely, low NDVI values may highlight areas with sparse vegetation or drought-stressed plants, which could influence fire behavior differently. By monitoring changes in NDVI over time, fire managers can track seasonal

vegetation growth, identify fuel accumulation patterns, and predict where wildfires are most likely to ignite and spread rapidly. This information allows for proactive measures such as targeted fuel reduction treatments, prescribed burns, and strategic deployment of firefighting resources to mitigate fire risk and protect vulnerable areas effectively. Therefore, NDVI plays a crucial role in wildfire prediction, planning, and response by providing actionable insights into vegetation conditions and fire potential across landscapes.

Obtaining NDVI (Normalized Difference Vegetation Index) data for all seasons of an area is highly beneficial for gaining comprehensive insights into wildfire management and mitigation strategies. NDVI data across seasons provides a detailed temporal perspective on vegetation dynamics, highlighting seasonal variations in vegetation density, health, and moisture content. This information is crucial for assessing fuel loads, the amount and flammability of vegetation available to burn across different times of the year. This data can be crucial for future wildfire prevention planning and it should be noted that many areas are prone to wildfires because of their high fuel load. Below the algorithm for the calculation of NDVI is presented:

$$Normalised\ Difference\ Vegetation\ Index\ (NDVI) = \frac{(NIR-RED)}{(NIR+RED)}$$

2.10. Sentinel 2 images

The Sentinel 2 satellite is part of the European Space Agency's (ESA) Copernicus program, formerly known as GMES (Drush et al., 2012), designed to provide high-resolution optical imagery for various Earth observation applications. Sentinel 2 carries a multispectral sensor capable of capturing images in 13 spectral bands, ranging from visible to shortwave infrared wavelengths. Sentinel 2 is a constellation of two polar-orbiting satellites that deliver multispectral data at spatial resolution of up to 10m in the visual and near infrared bands and a great thematic resolution at 20 and 60 m spatial resolution, and with a revisiting frequency of 5 days. Table 1 shows the spectral and spatial characteristics of Sentinel 2 images.

These images are instrumental in monitoring and preventing wildfires due to their ability to provide detailed and frequent observations of vegetation conditions and land cover dynamics. These images can detect changes in vegetation health and density, which are crucial indicators of wildfire fuel availability and susceptibility. By analyzing Sentinel 2 data over time, fire managers can monitor vegetation growth patterns, identify areas of high biomass accumulation (potential fuel sources), and assess vegetation stress due to factors like drought or disease, all of which influence wildfire behavior. Moreover, the satellite's multispectral capabilities allow for the detection of subtle changes in land surface temperatures and moisture content, which are critical factors in fire spread and intensity. This information enables early detection of fire-prone areas and supports proactive wildfire prevention measures such as fuel management strategies (e.g., prescribed burns, fuel breaks) and emergency response planning. By integrating Sentinel 2 imagery into wildfire management workflows, authorities can enhance preparedness, response efficiency, and community safety in fire-prone region.

Table 1. Spectral and Spatial characteristics of Sentinel 2 images.

Spectral Band	Band description	Wavelength range (nm)	Spatial Resolution (m)
Band 1	Coastal aerosol	433–453	60
Band 2	Blue	458–523	10
Band 3	Green	543–578	10
Band 4	Red	650–680	10
Band 5	Red Edge 1	698–713	20
Band 6	Red Edge 2	733–748	20
Band 7	Red Edge 3	773–793	20
Band 8	Near Infrared	785–900	10
Band 8A	Narrow Near Infrared	855–875	20
Band 9	Water vapour	395–955	60
Band 10	Shortwave infrared-Cirrus	1360–1390	60
Band 11	Shortwave infrared 1	1565–1655	20
Band 12	Shortwave infrared 2	2100–2280	20

2.11. Planet image

Planet Labs, a private Earth imaging company, operates a fleet of small satellites known as CubeSats, which capture high-resolution, frequently updated satellite imagery of the entire planet. These satellites, collectively called the PlanetScope constellation, consist of hundreds of small, lightweight satellites that provide daily coverage of the Earth's landmass. Planet's imagery is valuable for a wide range of applications, including agriculture, forestry, environmental monitoring, urban planning, and disaster response. With resolutions ranging from 3 to 5 meters, Planet's satellite images offer detailed views that help track changes in land use, monitor crop health, assess the impacts of natural disasters, and support climate change research. The frequent revisits and high temporal resolution of Planet's imagery make it a crucial tool for timely and accurate geospatial analysis, enabling users to make informed decisions based on up-to-date visual data of the Earth's surface. Table 2 shows the spectral and spatial characteristics of Planet images. It is crucial to note that Planet images differ from Sentinel 2 satellite images. Planet images lack mid-infrared channels, resulting in lower spectral analysis capabilities and a reduced ability to identify features with high discriminative power compared to Sentinel 2. Nonetheless, Planet images offer a significantly higher spatial resolution (3m) than Sentinel 2, enabling more precise delineation of vegetation polygons during the segmentation phase. Therefore, the combined use of both types of satellite images is an important factor for the analysis of an area.

Table 2. Spectral and Spatial characteristics of Planet images.

Spectral Band	Band description	Wavelength range (nm)	Spatial resolution (m)
Band 1	Coastal blue	431–452	3
Band 2	Blue	465–515	3
Band 3	Green 1	513–549	3
Band 4	Green 2	547–583	3
Band 5	Yellow	600–620	3
Band 6	Red	650–682	3
Band 7	Red Edge	697–713	3
Band 8	Near Infrared	845–885	3

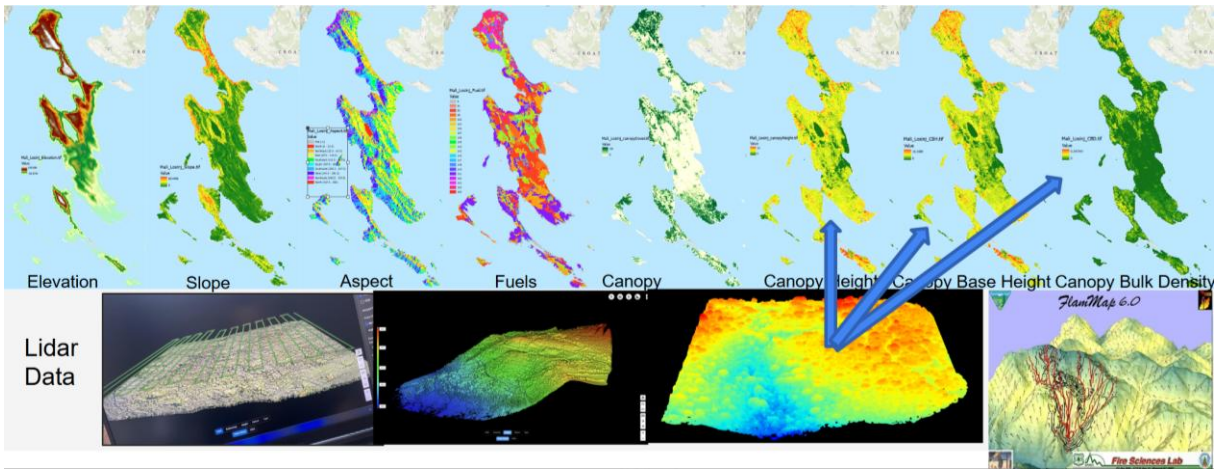

Figure 2. Fire Risk Assessment – Estimation of fire behaviors parameters

3. Fuel Mapping Methodological Approach

A clear and effective approach to fuel mapping is essential for understanding and managing wildfire risk. This section briefly outlines the main methods, data sources, and analytical techniques used to classify and map fuels across the pilot areas, highlighting how different approaches work together to deliver accurate, high-resolution results.

Fuel mapping will be done using Object-Based Image Analysis (OBIA), which is a technique used in remote sensing for image classification and analysis. Unlike traditional pixel-based approaches, OBIA groups pixels into meaningful image objects based on their spectral characteristics. These objects, or segments, are then classified and analyzed according to predefined rules and criteria set by the user. The initial step of OBIA involves creating objects based on the spectral similarity of adjacent pixels. The level of uniformity within each object is determined by the user through an appropriate scale parameter (Bock et al., 2005). Typically, in the final stage of classification, neighboring objects of the same class are merged.

OBIA, as implemented in the software eCognition, offers several advantages over traditional pixel-based methods when applied to High Spatial Resolution data. It effectively addresses within-class variability, and since classification occurs at the object level rather than the pixel level, it allows the use of various shape, texture, and context characteristics in the classification process (Kim et al., 2009; Rittl et al., 2013). Additionally, OBIA prevents the pixelated (salt and pepper) appearance often seen in pixel-based approaches, and the final classification results can be seamlessly integrated into a vector-GIS for further analysis. (Bock et al., 2005).

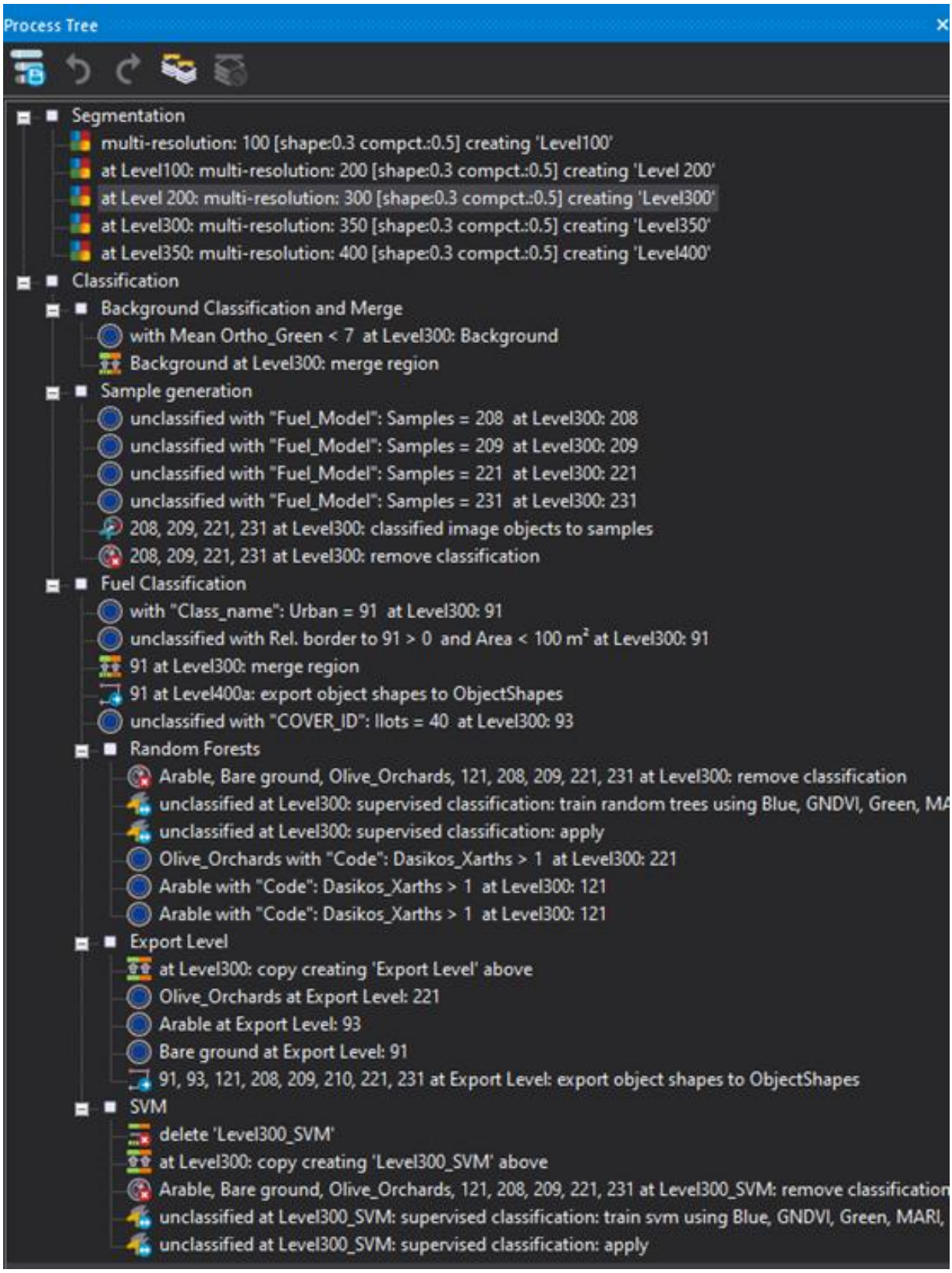

Figure 3. OBIA Classification Algorithm.

Another advantage of OBIA, compared to alternative pixel-based methods, is that in the same analysis data with different spatial resolutions can be

integrated. Furthermore, ancillary spatial data, such as the ones presented in the previous chapters can also be integrated in the analysis in order to improve the final spatial and thematic accuracy of the produced data. For the needs of the current project Sentinel 2 and Planet data will be integrated. The former, have high spectral resolutions and they probably constitute the best data for large scale mapping, at no cost. The latter have a much better spatial resolution, so they allow a better delimitation of the segments. The combination of the two types of images has been proved extremely effective in fuel and vegetation mapping. Various classifiers will be tested and evaluated for their accuracy, while the entire classification process will be assisted by ground truth data that will be collected by PP9 and all pilot partners. The classification is applied through a set of rules as shown in Figure 3.

4. Fire Risk Assessment Methodological Approach

A robust fire risk assessment is a key component of the project's overall methodology. This section briefly explains how various models, indices, and spatial data are integrated to evaluate wildfire hazard, combining factors like fuel conditions, human activities, past fire history, and fire behaviour simulations to identify the areas most at risk.

An in-depth analysis of fire risk assessment is essential for this project and therefore should be included in this paper. The Fire Danger Index (FDI) developed by Xofis et al. (2020a, b) will be utilized, incorporating two key components of the fire regime: fuel availability and burnability, and anthropogenic activities. Additionally, it includes the pyric history to indicate an area's potential vulnerability. Fuel availability will be assessed through a combination of remote sensing data, field data on vegetation structure, and compositional characteristics. Anthropogenic activities will be factored into the FDI by considering the proximity to the nearest road or settlement. The pyric history will be integrated by collecting data from local forest services and converting it into a Raster GIS format.

The FlamMap model can be utilized to simulate fire behavior. FlamMap is a two-dimensional fire simulation model that estimates fire behavior under uniform weather conditions. It calculates key components of fire behavior, including fireline intensity, rate of spread, flame height, and crown fire activity. Although FlamMap does not account for ignition points or changing weather conditions during a fire event, it is a powerful tool commonly used to estimate fire risk based on vegetation and topographic characteristics (Calkin et al. 2010). In this context, it is more suitable for this study compared to other simulators like FARSITE, as it allows for the identification of areas with a high potential for high-intensity fires under appropriate weather conditions. Fire behavior simulation using FlamMap generates a number of different parameters of fire behavior including fireline intensity (often called Byram's intensity), rate of spread, flame length e.t.c. Fireline intensity describes the heat release per meter of fire front and is calculated by the following equation which is an adjustment of the original equation developed by Byram:

$$I = 0.007\, H \cdot W \cdot R$$

where:

I=Fireline intensity in Kw/m, H=Heat yield in cal/g, W=Fuel loading in tonnes/ha and R=Rate of spread in m/min.

Fireline intensity estimates will be rescaled to a range between 0 and 1 to create the Fire Intensity (FI) component of the Fire Danger Index (FDI) formula (1). Rate of Spread (ROS) is also a crucial component of fire behavior, as it significantly influences the time needed for an ignition to develop into a large, difficult-to-suppress wildfire. Preliminary analysis in two study areas revealed that fireline intensity and rate of spread are significantly and positively correlated, with a correlation of approximately 60%. However, certain land cover types, such as grasslands and meadows, exhibit low energy release due to their low fuel load but still have a high ROS. In a complex landscape mosaic like the pilot area of Croatia and the broader Mediterranean region, these land cover types pose a high fire hazard because they increase the likelihood of a wildfire spreading rapidly into nearby areas with high fuel load and high potential for intense fires. Given that the FDI's purpose is to identify areas most vulnerable to high-intensity wildfires and to improve the organization of suppression forces, the ROS is included as a separate component in the FDI formula with a relatively low weight, despite already being a part of the fireline intensity equation. ROS values were also rescaled to a range between 0 and 1 to form the ROS component of the FDI formula.

$$FDI = 0.5 \cdot FI + 0.2 \cdot ROS + 0.2 \cdot HI + 0.1 \cdot PH$$

This formula also incorporates two additional critical components of fire risk: the Human Index (HI) and the Pyric History Index (PH), both serving as proxies for fire ignition probability. The HI captures the fire risk will be associated with human activities, using the distance to roads as a proxy. Values range from 0, for areas 200 meters or more away from roads, to 1 for areas in immediate proximity, as closer distances have been linked to higher ignition frequency (Ricotta et al. 2018; Catry et al. 2009). The PH, while not directly related to fire hazard, since past fires may reduce fuel load and thus fire intensity, provides insights into fire patterns linked to specific land uses and locations. For example, in the eastern Mediterranean, where free-range pastoralism is common, deliberate fires set by shepherds to improve grazing conditions create a pattern of clustered past fires, indicating higher fire risk areas. Although these fires are typically low-intensity due to their occurrence in autumn and in low-fuel areas, they still pose a risk of spreading to more flammable ecosystems. Including the PH index helps identify areas with specific patterns of past fires. The PH will be calculated using ignition data, applying a Kernel Density Estimation Function to convert point data into a raster file, with values from 0 (far from past ignition points) to 1 (close to past

ignition points). The resulting FDI ranges from 0 to 1, with higher values indicating greater fire hazard.

The fire risk assessment is closely tied to accurately mapping the biomass, which includes the fuel component. Therefore, precise mapping of fuel dispersion is crucial. The initial step in this process involves identifying the fuel models present in the study area. Using field-collected data, each of the samples will be assigned a fuel model that best represents its biomass characteristics. Based on field observations, collected data, and international literature on Mediterranean vegetation types, fuel models will be determined.

Ancillary data will be utilized to delineate agricultural and urban areas, while the tree cover density data will also be used. The classification process will be supported by ground truth data that will be collected. Additionally, sample data will be gathered through the visual inspection of VHR (Very High Resolution) aerial photographs. Various classifiers will be tested for their effectiveness in identifying the selected fuel models. The performance of each classifier will be evaluated based on its efficiency in accurately reproducing the training set. The classification will happen through the use of OBIA and also the Canopy Height Model (CHM) for each polygon will also be utilized while Canopy Base Height (CBH) will be assigned to each polygon based on the nearest sampled point and Crown Bulk Density will be computed in arc fuels. Consequently, five raster datasets will be produced, which are essential for implementing fire simulations.

The generated raster data, along with the Digital Elevation Model (DEM), the aspect model and the slope model, will be utilized in the fire simulation model FlamMap (Finney, 2006) to estimate potential Fireline Intensity and fire Rate of Spread. The study aims to evaluate fire hazard in the area in a spatially explicit manner under conditions favoring high-intensity fires. Recent major fires in the Eastern Mediterranean region, such as in Evros, Greece, occurred during the summer of 2023, the hottest on record for the area, marked by three consecutive heatwaves from June to August and wind patterns conducive to fire spread and intensity (Founda & Giannakopoulos, 2009; Tolika et al., 2009). Given the likelihood of such extreme weather events becoming more frequent in the future rather than remaining exceptionally rare, fire behavior simulations should be conducted under an extreme scenario with wind speeds of 35 km/h, assuming a prevailing south wind during summer. Fuel moisture parameters will be set at 3%, 4%, 5%, 30%, and 60% for 1-hour, 10-hour, 100-hour, live-woody, and live-herbaceous fuels, respectively.

5. Weather forecast data

Reliable weather forecast data is critical for supporting accurate fire danger assessments and planning. This section outlines the criteria used to select suitable datasets, explains the chosen MISTRAL platform and its COSMO models, and describes how these forecasts will be processed and integrated into the project's wildfire risk and warning systems.
For the characterization of the project's study areas, an in-depth search was made of the available weather forecast datasets covering the whole EU Mediterranean area. The dataset to be used was selected according to the following criteria:

- Geographical coverage: the dataset should possibly cover all the study areas included in the partner countries. The use of a unique dataset for the entire area would allow a harmonization of the data both in terms of data acquisition methods and for the climatic variables considered;
- Geometric resolution: the dataset should have sufficient geometric resolution (pixel size) to express the local variability of the weather-climate data;
- Climatic variables available in the dataset, both to be able to better characterize the areas of interest from a climatic point of view, and for the variables to be such that they can be used for a possible subsequent processing of the FWI (Canadian Forest Fire Weather Index);
- Availability of forecast data: the climate dataset had to be able to provide the forecast data for the next day, so that the calculation of FWI could take place the day before for the following day in such a way as to function as a "fire danger" warning system on the basis of the weather trend;
- Data quality: Recognition of the dataset by international bodies of meteorological data studies, and use of the dataset by local authorities and organizations were taken into account;
- Availability of an open API (Application Programming Interface) service, in order to be able to integrate such data within FRED platform programmatically.

The selected weather forecast datasets are those provided by the Meteo Italian Supercomputing Portal - MISTRAL (https://www.mistralportal.it/), a project co-funded by the EU aimed to build an Italian open weather data platform to provide national and international citizens, public administrations, and private organizations with weather data from

observational networks, historical and real-time analysis and forecasts. Since 2021, the European Centre for Medium-Range Weather Forecasts (ECMWF) extracts regional observational data available in real-time from the MISTRAL Meteo-Hub. These data are used by ECMWF in the assimilation phase for numerical forecast models, thus increasing the observational database used until now. The use of observational data by ECMWF testifies to the added value that regional observational weather data acquire through sharing on Meteo-Hub.

More specifically, MISTRAL offers two types of datasets of interest to FRED:

- **COSMO-5M** (COSMO at 5km – Mediterranean Region), a numerical integration of the forecast model called COSMO with a 5 km grid covering the whole Mediterranean Europe, thus including all FRED pilot areas. It includes two runs per day (00 and 12 UTC) of 18-hour assimilation (including the repetition of the last 6 hours of the previous run) and two runs per day (00 and 12 UTC) of 72-hour forecast and
- **COSMO-2I** (COSMO at 2.2km – Italy area), another numerical integration of the forecast COSMO model with a 2.2 km grid which covers not only the entire Italian territory, but also part of the countries facing the Adriatic Sea. In particular, all FRED pilot areas are covered by this dataset with the only exception of Portuguese one. It also represents a numerical integration of the COSMO forecast model. The procedure includes two runs per day (00 and 12 UTC) of 48-hour forecasts.

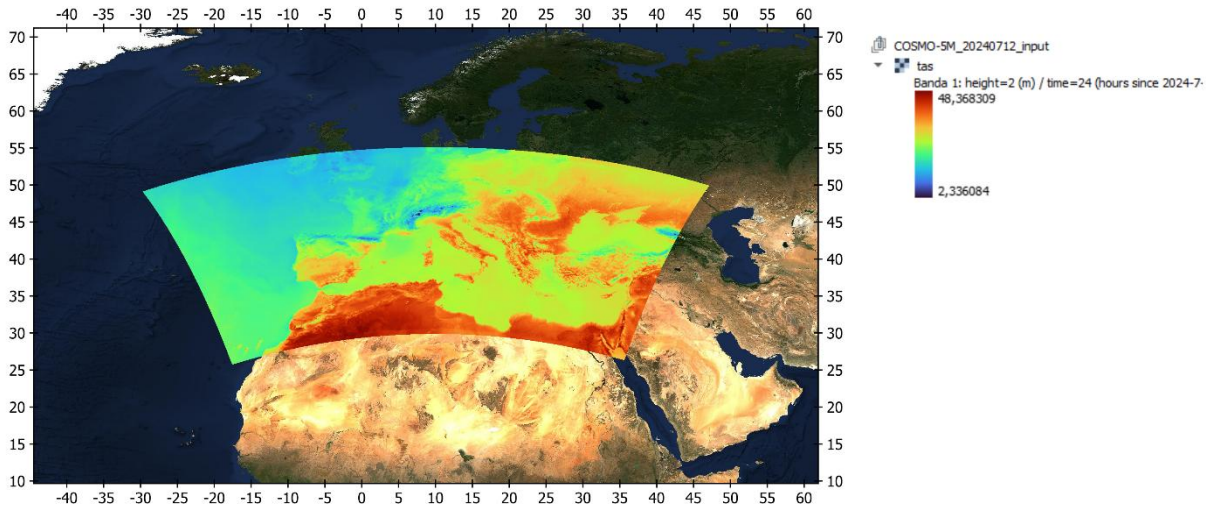

Figure 4. COSMO-5M: Forecasted Air temperature (°C) at noon on 12 July, 2024.

To get an idea of the geographical coverage of COSMO-5M weather forecast dataset, look at the Figure 4.

5.1. How to download the MISTRAL forecast data using the APIs

The forecast datasets for every day of the last week and for two runs per day are released as open data in the GRIB (General Regularly distributed Information in Binary form) format, a WMO (World Meteorological Organisation) standard format. To download them, users can directly use the following Meteo-Hub APIs:

- To get the list of all GRIB files for a specific dataset:

```
GET https://meteohub.mistralportal.it/api/datasets/{dataset_name}/opendata
```

  where the query parameter `dataset_name` is the name of the dataset of which the packages list is referred (e.g., `COSMO-2I` or `COSMO-5M`).

- To ask for download a specific GRIB file (whose filename is known):

```
GET https://meteohub.mistralportal.it/api/opendata/{filename}
```

  where the query parameter `filename` is the name of the package to download (e.g., `data-20240526T190845Z-93c81644-a741-4981-b293-02f2ae2a56ee.grib`)

- To ask for download one or more GRIB files related to a specific dataset, a specific reference date and/or a specific run (without knowing the filename):

```
GET
https://meteohub.mistralportal.it/api/opendata/{dataset_name}/download?reft
ime={reference_date}&run={run}
```

  where the query parameter `dataset_name` is the name of the dataset of which the packages download is requested (e.g., `COSMO-2I` or `COSMO-5M`), the `reference_date` parameter can be expressed with the following data formats: YYYYMMDD or YYYY-mm-dd where YYYY stays for year, mm for month and dd for day (e.g., `20240526` or `2024-05-26`), and finally the `run` parameter in the time format HH:MM, where HH stays for hour and MM stays for minutes (e.g., `12:00`). The time for run parameter is intended as UTC.

No authentication is required to use these previously described APIs, unless the request of open data download refers to a dataset with restricted access.

Source: https://www.mistralportal.it/user-guide/#jump-api (accessed 11/07/2024).

5.2. Meteorological variables of interest

Among the meteorological variables included in the COSMO-5M and COSMO-2I datasets, there are the following hourly forecast data:

- Air temperature [°C] at 2 m;
- Dew point temperature [°C] at 2 m;
- u-component of wind [m/s] at 10 m;
- v-component of wind [m/s] at 10 m;
- Total precipitation [kg/m^2].

These forecast data could be used to calculate the relative humidity, the wind speed, as well as the 24 h-cumulated precipitation at noon, which together with the air temperature at noon are the input meteorological variables for the calculation of the FWI, unless the initial condition.

5.3. How to retrieve the FWI input parameters from MISTRAL data

To retrieve the input meteorological variables for the FWI calculation it is necessary to extract and process the preliminary variables from the GRIB file. For instance, in Windows Subsystem for Linux (WSL), we can download the data of our interest (e.g., COSMO-2I forecast data related to 21/06/2024, run at 12:00) by executing the following API:

```
wget --content-disposition \
"https://meteohub.mistralportal.it/api/opendata/COSMO-
2I/download?reftime=20240621&run=12:00"
```

To extract the input data for the calculation of FWI on the day following the day of the forecast, the use of specialized packages and libraries as ecCodes, CDO and xclim is recommended. To this aim, we can create a Conda environment (e.g., `mistral-env`) and install the requirements:

```
# Create and activate a conda environment
conda create -n mistral-env
conda activate mistral-env

# Install packages
conda install -c conda-forge python-eccodes cdo xclim gdal
```

it is possible to execute the following bash script (e.g., `grib2nc.sh`):

```
#!/usr/bin/env bash

# input parameters
```

```
GRIB=$1
PREFIX=$2
DATA_FOLDER=data

mkdir -p $DATA_FOLDER
cd $DATA_FOLDER

echo Filtering GRIB messages into separate GRIB files...
grib_copy $GRIB -w stepRange=24 "[shortName]_[stepRange].grib"

echo Converting 2m temperature...
cdo -f nc \
    -setattribute,tas@standard_name="air_temperature",tas@long_name="noon
temperature",tas@units="degC",tas@cell_method="time: point" \
    -subc,273.15 \
    -chname,var11,tas \
    2t_24.grib temp.nc

echo Calculating 10m wind speed...
grib_copy -M 10u_24.grib 10v_24.grib wind_components.grib
cdo -f nc \
    -setattribute,u10@standard_name="eastward_wind",u10@long_name="u-
component of wind at
10m",u10@units="km/h",v10@standard_name="northward_wind",v10@long_name="v-
component of wind at 10m",v10@units="km/h" \
    -mulc,3.6 \
    -chname,var33,u10,var34,v10 \
    wind_components.grib wind_components.nc
xclim -v -i wind_components.nc -o wind.nc wind_speed_from_vector --uas u10
--vas v10

# filter total precipitation
grib_copy -w shortName=tp,stepRange=0-1/1-2/2-3/3-4/4-5/5-6/6-7/7-8/8-9/9-
10/10-11/11-12/12-13/13-14/14-15/15-16/16-17/17-18/18-19/19-20/20-21/21-
22/22-23/23-24 $GRIB tp_0-24.grib

echo Calculating 24h total precipitation...
cdo -f nc \
    -setattribute,pr@standard_name="precipitation_flux",pr@long_name="24-
hour precipitation",pr@units="mm/d",pr@cell_method="time: sum(interval: 1
day aggregation: sum)" \
    -chname,var61,pr \
    -shifttime,30minutes \
    -daysum \
    -shifttime,11hours \
    tp_0-24.grib prec.nc

echo Calculating relative humidity...
cdo -f nc \
    -setattribute,tas@standard_name="air_temperature",tas@long_name="noon
air temperature",tas@units="degK",tas@cell_method="time:
point",tdps@standard_name="dew_point_temperature",tdps@long_name="noon dew
point temperature",tdps@units="degK",tdps@cell_method="time: point" \
    -chname,var11,tas,var17,tdps \
    temperatures.grib temperatures.nc
xclim -v -i temperatures.nc -o rh.nc hurs_fromdewpoint --tas tas --tdps
tdps --method 'sonntag90'

echo Merging NetCDF files...
cdo -O merge temp.nc wind.nc prec.nc rh.nc ${PREFIX}_input.nc
```

```
# clean temporary data
rm tp*.grib *_24.grib temp*.* wind*.* prec.nc rh.nc lat*.nc out*.nc *.txt
```

```
# Run the grib2nc.sh script
./grib2nc.sh ~/mistral/data/data-20240621T175426Z-e55f2100-81ad-4e19-8019-
2624acf5366e.grib COSMO-2I_20240622
```

The Coordinate System (CS) in which the gridded forecast data are represented is a rotated latitude longitude CS with the following Well-Known Text (WKT):

```
GEOGCRS["Coordinate System imported from GRIB file",
    BASEGEOGCRS["Coordinate System imported from GRIB file",
        DATUM["unnamed",
            ELLIPSOID["Sphere",6367470,0,
                LENGTHUNIT["metre",1,
                    ID["EPSG",9001]]]],
        PRIMEM["Greenwich",0,
            ANGLEUNIT["degree",0.0174532925199433,
                ID["EPSG",9122]]]],
    DERIVINGCONVERSION["Pole rotation (GRIB convention)",
        METHOD["Pole rotation (GRIB convention)"],
        PARAMETER["Latitude of the southern pole (GRIB convention)",-47,
            ANGLEUNIT["degree",0.0174532925199433,
                ID["EPSG",9122]]],
        PARAMETER["Longitude of the southern pole (GRIB convention)",10,
            ANGLEUNIT["degree",0.0174532925199433,
                ID["EPSG",9122]]],
        PARAMETER["Axis rotation (GRIB convention)",0,
            ANGLEUNIT["degree",0.0174532925199433,
                ID["EPSG",9122]]]],
    CS[ellipsoidal,2],
        AXIS["latitude",north,
            ORDER[1],
            ANGLEUNIT["degree",0.0174532925199433,
                ID["EPSG",9122]]],
        AXIS["longitude",east,
            ORDER[2],
            ANGLEUNIT["degree",0.0174532925199433,
                ID["EPSG",9122]]]]
```

Save the WKT as text file (e.g., `grib_cs.wkt)` in the same folder containing data. Finally, it is possible to use the `gdalwarp` utility program of the GDAL library to transform the forecast data from the rotated lat-lon CS to another CS (e.g., geographic lat-lon, EPSG:4326) and convert data to another format (e.g., GeoTIFF), as follows:

```
# Air temperature (degC) at noon
gdalwarp -tr 0.02 0.02 -s_srs grib_cs.wkt -t_srs EPSG:4326 NETCDF:"COSMO-
2I_20240622_input.nc":tas COSMO-2I_20240622_temperature.tif

# Wind speed (km/h) at noon
gdalwarp -tr 0.02 0.02 -s_srs grib_cs.wkt -t_srs EPSG:4326 NETCDF:"COSMO-
2I_20240622_input.nc":sfcWind COSMO-2I_20240622_wind_speed.tif

# 24h-cumulated precipitation (mm) at noon
gdalwarp -tr 0.02 0.02 -s_srs grib_cs.wkt -t_srs EPSG:4326 NETCDF:"COSMO-
2I_20240622_input.nc":pr COSMO-2I_20240622_24h_precipitation.tif

# Relative humidity (%) at noon
gdalwarp -tr 0.02 0.02 -s_srs grib_cs.wkt -t_srs EPSG:4326 NETCDF:"COSMO-
2I_20240622_input.nc":hurs COSMO-2I_20240622_relative_humidity.tif
```

The COSMO-2I Air temperature and Relative humidity at noon are represented in Figure 5, while 24-h precipitation and Wind speed at noon in Figure 6.

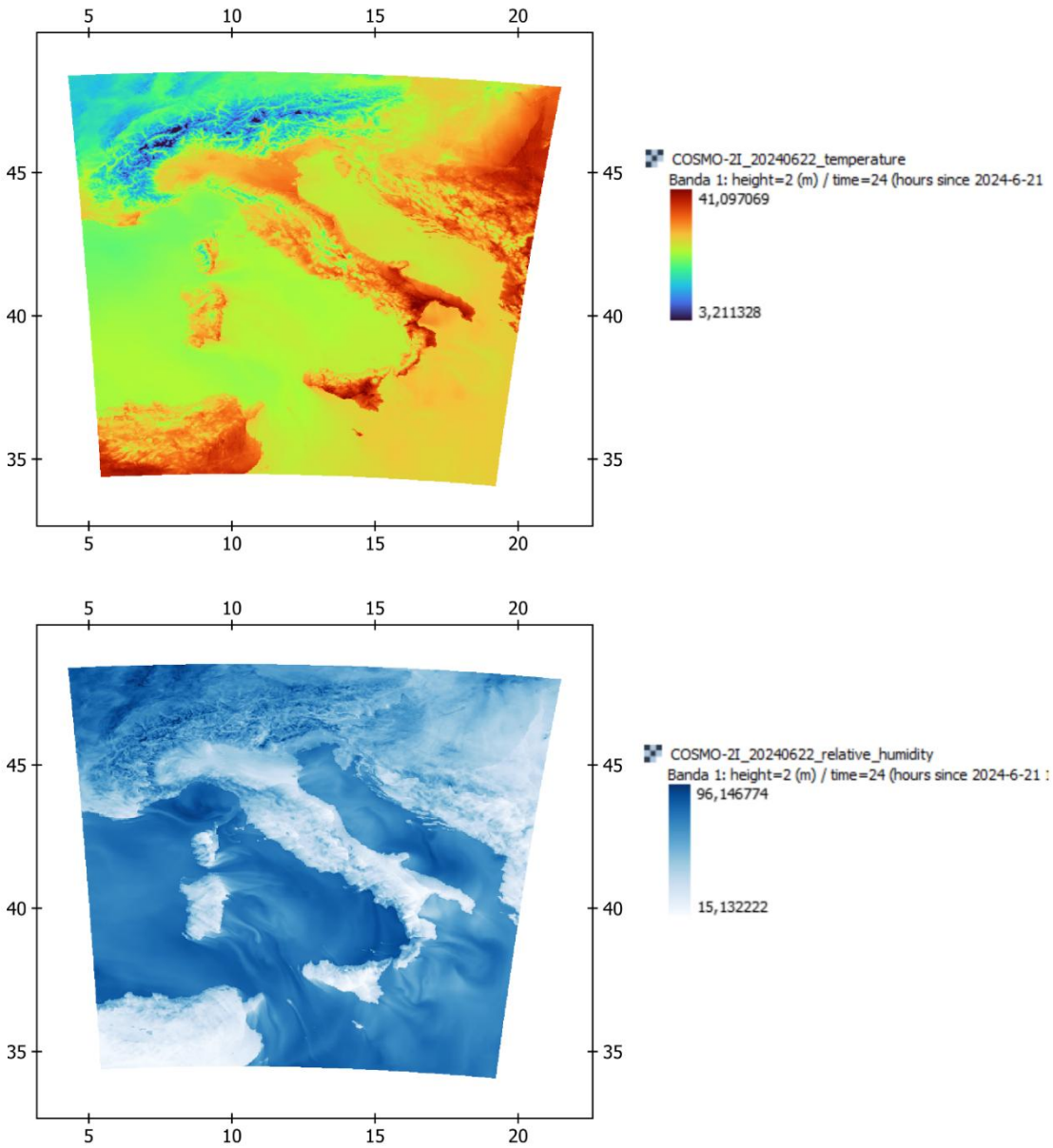

Figure 5. COSMO-2I: Air temperature and Relative humidity forecasted at noon on 22 June, 2024.

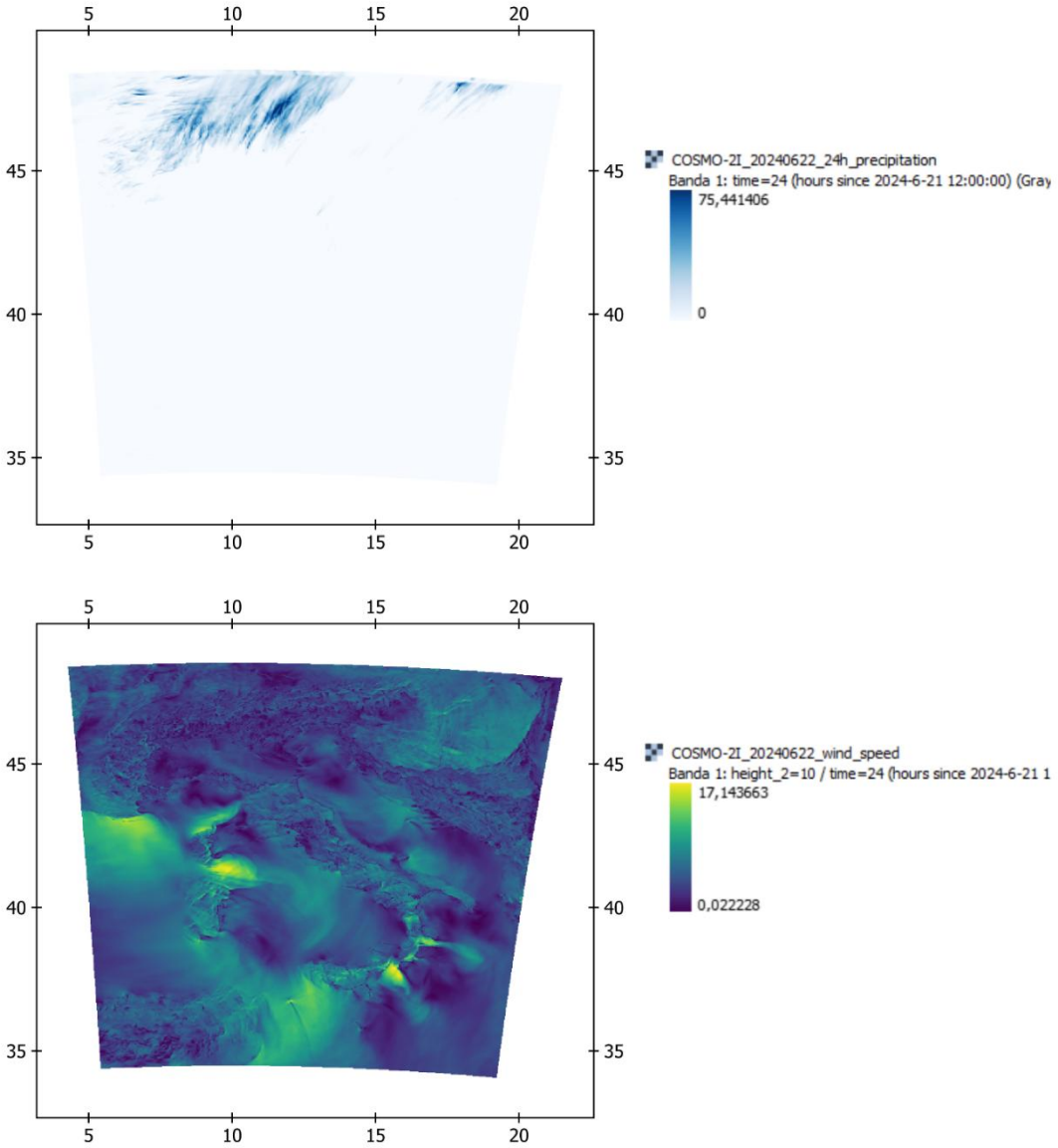

Figure 6. COSMO-2I: 24-h precipitation and Wind speed at noon on 22 June, 2024.

6. UAS application for data collection

This chapter provides an overview and features of the key UAS payloads and sensors, outlines the main data collection techniques and mapping approaches, and highlights how these systems enhance operational capabilities through real-time data transmission and advanced mission actions. Special attention is given to the interoperability of these techniques and their practical applications within the FRED project's operational framework.

6.1. Payloads

UAS have revolutionized various industries by integrating advanced sensor technologies. These sensors can be broadly categorized into visual and non-visual payloads. Visual sensors in the UAS domain means RGB visual cameras, LiDAR sensors, infrared cameras, and multispectral cameras, each serving unique purposes in different applications. Non-visual payloads encompass equipment such as RTK modules, loudspeakers, microphones, spotlights, parachutes, and Software Development Kits (SDK), i.e., any additional payload unit that is not usually equipped with the UAS. All these mentioned payloads enhance the operational capabilities of UAS beyond visual data collection. Every concrete payload mentioned with its commercial name and specifications is exclusively produced by the UAS manufacturer. Third-party payloads that are compatible or can be made compatible with minor modifications will not be taken into account.

Visual sensors are essential for capturing detailed imagery and data for various applications. Here, we explore the strengths and limitations of key visual sensors mentioned above.

6.1.1. Visual RGB camera

RGB Visual cameras are the most common type of visual sensors used in Unmanned Aerial Systems (UAS). These cameras capture images and videos by detecting and recording light in three primary color channels: red, green, and blue. The combination of these three colors allows the camera to produce images in full color, replicating what the human eye typically perceives. RGB cameras are widely used across various industries due to their versatility and ability to provide high-resolution visual data. Some applicable versions of thermal cameras compatible with above mentioned UAS models are shown in following figure.

(a) (b) (c)

Figure 7. (a) DJI Zenmuse H30; (b) DJI Zenmuse H20; (c) DJI Zenmuse P1; Source: DJI webpage

RGB Visual cameras possess several strengths, including the ability to capture detailed and high-resolution images, making them ideal for tasks requiring precise visual documentation from aerial perspectives. They provide true color representation, which is crucial for applications where accurate color depiction is essential. Their versatility allows them to be used in various applications, such as general observation, mapping (photogrammetry, orthomosaics, etc.), inspection, photography, and videography. However, they have limitations, such as a heavy dependence on ambient light, which means poor lighting conditions like low light, fog, or shadows can significantly reduce image quality. They are limited to capturing only visible light and cannot detect information outside the visible spectrum, such as infrared or ultraviolet light. Furthermore, obstructions like dense foliage, smoke, or other barriers can impede the camera's ability to capture clear images. Despite these limitations, RGB cameras remain a vital component of UAS technology, evidenced by the fact that all UASs are equipped with at least one RGB visual camera.

6.1.2. Thermal camera

Thermal cameras, also known as infrared cameras, are sophisticated sensors used to detect infrared radiation and visualize heat differences. These cameras are essential in various applications such as search and rescue, firefighting, and industrial inspections because they can identify heat spots, monitor temperature variations, and detect structural issues invisible to RGB cameras. The key component of a thermal camera is a heat sensor attached to a special lens, which is adapted to work with standard image capture technologies.

Currently, the maximum sensor resolution for non-cooled thermal cameras, such as those carried by commercial UAVs, is 640 × 512. Thermal cameras capture infrared radiation that exists at wavelengths between visible light and microwaves, making it possible to visualize the otherwise invisible infrared spectrum. In a color thermographic display, warmer components

appear as reds, oranges, and yellows, while cooler areas show as violets and blues. High-resolution thermal cameras often have a 640x480px detector, delivering 307,200 pixels, compared to 76,800 pixels in a thermal imager with a 320 × 240px detector. Standard formats include 160x120px, 384288px, and 640x480px. For search and rescue missions, a 160x120px format requires flying at a maximum height of 30 meters (100 feet) to discern a victim effectively. The optimal format for such missions is at least 640x480px, allowing flight above 30 meters (100 feet) while maintaining visibility. While a 160x120px format is sufficient to visualize and locate a hot spot, a larger image format determines the scene size or range, with the larger the format, the greater the usable range of the camera. Some applicable versions of thermal cameras compatible with above mentioned UAS models are shown in following figure.

(a) (b) (c)

Figure 8. (a) DJI Zenmuse H30T; (b) DJI Zenmuse H20T; (c) DJI Zenmuse XT V2;
Source: DJI Webpage

Thermal imaging is particularly useful in dark environments, such as nighttime conditions, because the ambient temperature is often lower, allowing hot areas to stand out with higher contrast. These cameras are passive sensors that only detect heat differences, making them ideal for identifying heat sources regardless of the surrounding light conditions.

Modern thermal cameras can display real-time detection of minimum and maximum temperatures and allow for manual spot metering for specific temperature measurements. They offer several color palettes, such as White-Hot, Black-Hot, Rainbow, Ironbow, and Arctic, which are used for various tasks to enhance visualization and interpretation of thermal data. Despite their strengths, thermal cameras typically have lower resolution compared to RGB cameras and can be affected by reflective surfaces and atmospheric conditions. Accurate interpretation of thermal data requires specific skills and understanding of the context in which the camera is used.

6.1.3. Light Detection and Ranging sensor, LiDAR

LiDAR, short for Light Detection and Ranging, is a remote sensing technology that employs rapid laser pulses to create detailed three-

dimensional point maps also known as point clouds. The process involves three key steps:

- Emission: The LiDAR device emits a rapid pulse of laser light directed towards the target object.
- Reflection: The emitted light reflects off the object and travels back to the LiDAR sensor.
- Detection: The LiDAR sensor measures the time it takes for the light to return. Given that the speed of light is a constant, this time duration is used to calculate the distance between the sensor and the target object, allowing for the creation of precise 3D point maps.

Figure on LiDAR working principle is shown below.

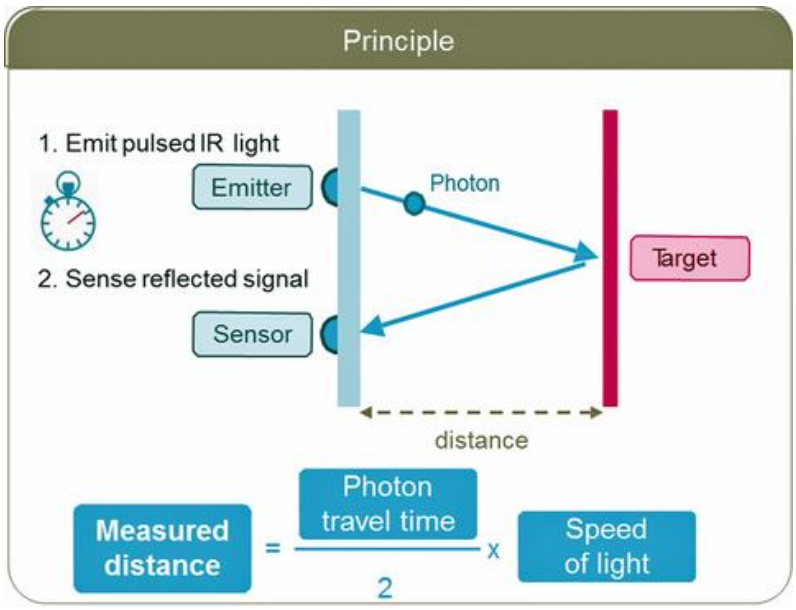

Figure 9. LiDAR principle.
Source: DJI site

Important components of LiDAR system are: LiDAR module GBSS receiver, IMU, Inertial Navigation System, INS.

Technical Details: LiDAR systems use lasers to emit pulses of light, with the wavelength of the laser determining its penetration capabilities and the types of reflections it can detect. Near-infrared (NIR) LiDAR typically uses lasers with wavelengths between 800 and 1,000 nanometers, ideal for forestry applications as they can penetrate vegetation and detect multiple returns from a single pulse. The detection range of a LiDAR system depends on factors such as laser power, receiver sensitivity, and object reflectivity.

(a) (b)

Figure 10. (a) DJI Zenmuse L2; (b) DJI Zenmuse L1;
Source: DJI Webpage.

LiDAR systems can capture multiple returns from a single pulse, allowing for detailed analysis of different layers within a scene. For example, the first return might capture the top of a tree, intermediate returns could capture branches, and the last return might capture the ground. This capability is crucial for applications like vegetation analysis, topographic mapping, and power line modeling, where understanding the structure at different levels is essential.

One of the key advantages of LiDAR is its ability to penetrate vegetation and provide accurate distance measurements, which is essential for creating detailed terrain models. This technology is also beneficial for capturing details of thin structures, such as power lines or roof edges, which are generally too small to be detected by other methods. LiDAR systems can operate well in low light or densely vegetated areas, ensuring accuracy in challenging conditions. They are ideal for projects where detail and precision are paramount, such as accident scene reconstruction, digital terrain modeling, and precision mapping.

Overall, LiDAR technology significantly enhances the capabilities of UAS by providing critical data for various advanced applications. Its ability to produce high-resolution, accurate 3D models and penetrate complex environments makes it an indispensable tool for modern surveying and mapping tasks

6.1.4. Multispectral camera

A multispectral camera is an imaging device that captures data at different wavelengths across the electromagnetic spectrum, including visible light and near-infrared (NIR). Unlike traditional RGB cameras that only capture red, green, and blue wavelengths, multispectral cameras can detect wavelengths beyond the visible spectrum. This ability allows them to capture more detailed and diverse information about the objects or scenes being imaged.

Multispectral cameras operate by using multiple sensors or a single sensor with a filter wheel to capture images at different wavelengths. They employ specialized optics to capture light across various spectral bands, including visible light (400-700 nm) and extending into the near-infrared range (700-2500 nm), depending on the application and camera design. These cameras are equipped with spectral filters that allow specific wavelengths to pass through while blocking others, arranged in a filter wheel or as an array over the sensor. Each filter corresponds to a particular spectral band, generating multiple images, each representing a different spectral band. These images are combined to form a multispectral dataset, providing detailed information about the reflectance properties of the scene or object. The multispectral data is analyzed using specialized software to interpret reflectance values at different wavelengths, revealing material composition, health, and other properties of the objects.

Applications of multispectral cameras are diverse, including agriculture (monitoring vegetation health, assessing crop conditions), environmental monitoring (tracking deforestation, water quality), forestry (managing forest inventories, detecting tree health issues), mining and geology (identifying mineral compositions, mapping geological features), and surveillance and security (enhancing surveillance with additional information like heat signatures). The strengths of multispectral cameras lie in their ability to provide detailed spectral information, versatility across various applications, and non-invasive monitoring. However, they can be expensive, require careful calibration, and the data analysis is complex, necessitating advanced software and expertise in remote sensing.

Figure 11. DJI Zenmuse X3.
Source: DJI Webpage

Non-visual payloads significantly expand the functionality of UAS providing additional capabilities that go beyond visual data collection. These payloads enable drones to perform a variety of specialized tasks in different environments and industries.

6.1.5. Loudspeaker

A loudspeaker integrated into a UAS is an audio output device used to broadcast messages from the drone.

They can deliver important information or instructions to the public, especially in areas where traditional public address systems might not reach, such as during large outdoor events or in remote locations. Law enforcement and security agencies utilize drones equipped with loudspeakers to manage crowds by issuing commands, warnings, or updates during events, protests, or emergencies, ensuring public safety and order. Additionally, during disasters or rescue operations, loudspeakers on drones can relay critical information to individuals in hard-to-reach or hazardous areas, guiding them to safety or informing them of necessary actions. This capability is crucial in scenarios where ground communication is compromised or delayed, providing timely and potentially life-saving information.

6.1.6. Spotlight

A spotlight on a UAS is a high-intensity light source designed to illuminate areas during low-light conditions.

Spotlights on UASs significantly enhance their operational capabilities, particularly during nighttime activities. They improve visibility for nighttime search and rescue missions, patrolling, and inspections, allowing operators to identify objects or individuals in dark environments. During infrastructure inspections, spotlights can illuminate hard-to-reach or poorly lit areas, such as under bridges or inside tunnels, ensuring thorough visual assessment. In security operations, drones equipped with spotlights can illuminate and monitor specific areas, deterring potential intruders and enhancing surveillance capabilities.

6.1.7. Real-Time Kinematic module

Real-Time Kinematics (RTK) module is a technology that enhances the accuracy of GPS data to centimeter-level precision, making it indispensable for applications that require high-precision positioning and navigation. Instead of the employment of PRN (code) ranging signal, the RTK technique is based on the use of carrier (phase) measurements.

Standard GPS systems, limited to meter-level accuracy due to atmospheric and signal errors, are supplemented by an RTK setup that includes a

stationary base station and a mobile receiver. The base station, with a known precise location, continuously receives satellite signals' code and phase measurements and calculates its position, identifying any errors. It then generates correction data, representing the discrepancy between its known and calculated positions, and transmits this data to the mobile receiver in real-time via radio, cellular network, or other communication methods. The mobile receiver, typically a drone, applies these corrections to its own satellite signal measurements, achieving highly accurate positioning. This corrected position data enables precise flight control and accurate data collection, essential for applications like surveying, mapping, and inspections where accuracy is critical.

6.1.8. Parachute

Parachutes are integrated as a safety mechanism to minimize damage in case of a system failure or emergency landing.

When a UAS experiences a malfunction or power loss, the parachute deploys automatically or via manual activation, significantly reducing the speed of descent and protecting the UAS from severe damage upon impact, thereby reducing the risk of injury or damage to people and property on the ground. UAS parachute systems can include spring-loaded mechanisms or compressed gas to quickly release the parachute, with sensors and onboard systems detecting free fall or critical failures to trigger the deployment. In some regions, using a parachute system can help UAS comply with aviation safety regulations, allowing them to operate in more areas and under more conditions.

6.1.9. Software Development Kit

Software Development Kit (SDK) are collections of software development tools and libraries that allow developers to create custom applications and functionalities. These SDKs are used to create custom applications and integrate specialized payloads with UASs, enhancing their versatility for specific tasks. SDKs are also used to program automated flight paths, data collection routines, and real-time processing functionalities such as delivering telemetry or any other data form UAS.

As a recap of the review of payloads that provide visual or non-visual output, the table below summarizes all compatibilities of industrial solution UAS

(currently available on the market) and payloads and leads to defining three acceptable UAS systems for professional and proficient purposes.

Table 3. Compatibility of payloads with the UAS system.

	DJI Matrice 350 RTK	DJI Matrice 30T	DJI Mavic 3T	DJI Mavic 2 Enterprise Advanced	DJI Phantom 4 RTK
Visual RGB Camera	X	X	X	X	X
Thermal Camera	X	X	X	X	
LiDAR	X				
Multispectral Camera			X[1]		X[2]
Loudspeaker	X*	X*	X	X	
Spotlight	X*	X*	X*	X	
Parachute	X*	X*	X*	X*	X*
RTK module	X	X	X	X	X
SDKs	X	X	X	X	X

X* Third-party payload solutions
[1] The UAS model DJI Mavic 3M (with similar characteristics to the DJI Mavic 3T) does not have a thermal camera but instead features a multispectral camera.
[2] The UAS model DJI Phantom P4 (with similar characteristics to the DJI Phantom RTK) is equipped with an integrated multispectral camera.

UAS (Unmanned Aerial Systems) data analysis software is designed to process and interpret the vast amounts of data collected by drones. These software platforms transform raw data into actionable insights, supporting various applications such as mapping, surveying, agriculture, and inspection. Key features typically include image processing, 3D modeling, real-time mapping, and analytical tools that enhance the capabilities of drones in professional and commercial settings. Here, we discuss some of the leading software tools in the industry: Pix4D, DroneDeploy, Agisoft Metashape, and DJI Terra.

6.1.10. Postprocessing data analysis software

Post-processing data analysis software is designed to process and interpret the vast amounts of aerial data collected by UAS, transforming raw data into actionable insights. These platforms support various applications such as mapping, surveying, inspection, and agriculture. Key features typically include advanced image processing, photogrammetry for creating 2D and 3D models, generating orthomosaics and point clouds, real-time mapping, and analytical tools that enhance the capabilities of drones in professional and commercial settings. They also offer features for volume measurement, and high-accuracy mapping using Ground Control Points (GCPs) and RTK data. A strong GIS base is integral to all these software platforms, enabling precise georeferencing and spatial analysis. Additionally, these software solutions enable mission planning and data capture, integrating seamlessly with GIS and CAD systems for further analysis. Users benefit from both cloud and desktop processing options, allowing flexibility and collaboration through sharing and viewing project data online. Here, identified some of the leading software platforms used in the industry: DJI Terra, Pix4D, Agisoft Metashape, and DroneDeploy.

6.2. Data collection techniques

UAS data collection techniques for aerial surveying and mapping represent efficient, accurate and cost-effective methods. Continuing to the previous subsection and description of methods and equipment, the key techniques employed in aerial surveying and mapping using UAS are 2D/3D Photogrammetry, Ortho-mosaic mapping, LiDAR, Multispectral and hyperspectral imaging, Thermal imaging, Real-time data transfer and live video streaming, Geometrical evaluation, and Mapping approaches (rectangle and spiral).

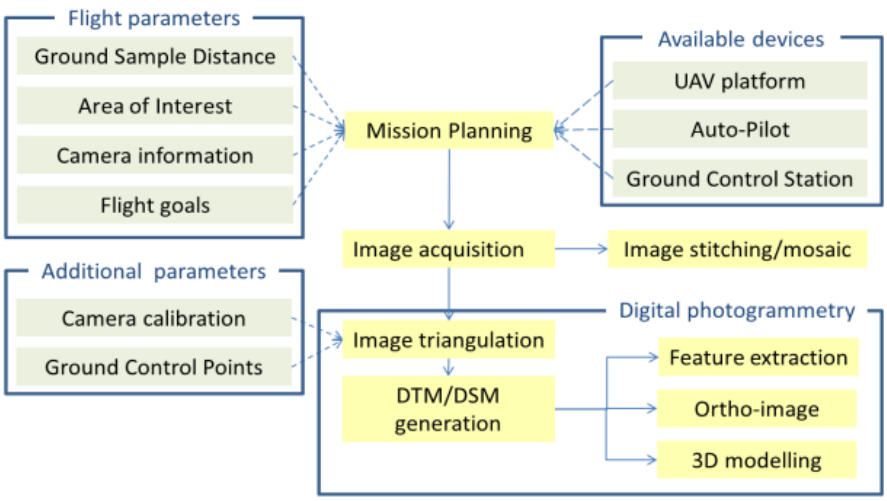

Figure 12. UAS data acquisition and processing: A general workflow (10.1007/s12518-013-0120-x)

6.2.1. 2D/3D Photogrammetry

Photogrammetry is a precise remote sensing technique that uses photographs to measure and map environments. It involves capturing images from different perspectives to create accurate representations of objects and landscapes. This method is commonly used in surveying, mapping, architecture, engineering, and environmental monitoring. Photographs are taken using aerial, satellite, or ground-based cameras, with drones often employed for their efficiency in covering large areas. Georeferencing aligns images with real-world coordinates using GPS data, ensuring spatial accuracy. Specialized software processes the images to generate point clouds, digital elevation models (DEMs), orthomosaics, and 3D models. Techniques like Structure from Motion (SfM) and Multi-View Stereo (MVS) are commonly used. Depending on the application, various corrections and enhancements may be applied to improve data accuracy and usability.

Photogrammetry is used for topographic mapping, architectural surveys, environmental monitoring, and infrastructure inspection. It offers high precision, rapid data collection, and versatility across different fields and scales. Tools involved include high-resolution digital cameras and software such as Agisoft Metashape, Pix4D, and Autodesk ReCap. This technique is critical in geospatial sciences, providing accuracy and efficiency in mapping and measurement tasks, especially when integrated with UAS technologies.

The 2D Photogrammetry technique involves capturing overlapping images of an area from the air to create 2D maps. The UAS flies in a grid pattern, capturing high-resolution images. These images are then processed using

photogrammetry software to generate orthophotos (i.e. geometrically corrected images).

The 3D Photogrammetry technique is similar to the previous one, but it extends to create 3D models od terrain and structures. By capturing images from multiple angles with overlapping fields of view, photogrammetry extracts depth information to create 3D models from 2D images.

Photogrammetry data can be easily integrated with other GIS (Geographic Information Systems) data and software. Outputs such as orthophotos and 3D models are compatible with various mapping and CAD (Computer-Aided Design) tools.

6.2.2. Ortho-mosaic Mapping

Ortho-mosaic mapping involves creating a seamless, high-resolution map from multiple aerial images. Images are geometrically corrected for distortion and stitched together to form a single, continuous map. Ortho-mosaic maps are produced in standard formats like GeoTIFF, which can be used across different GIS platforms and applications. They are also compatible with photogrammetric software and tools used in urban planning, agriculture, and environmental monitoring.

6.2.3. LiDAR

LiDAR uses laser pulses to measure distances to the Earth's surface, creating detailed 3D maps. A LiDAR sensor mounted on the UAS emits laser pulses and measures the time it takes for them to return after hitting the ground. The data is processed to create a dense point cloud representing the terrain. LiDAR data is widely used and can be integrated with photogrammetry data to enhance accuracy. It is compatible with various GIS, CAD, and BIM (Building Information Modeling) systems, making it useful for topographic mapping, forestry, and flood risk assessment.

In the framework of the activities foreseen by the FRED project, the use of remote sensing data from passive sensors such as Landsat and Sentinel-2 can explain a certain fraction of surface fuel load variability, as they carry information related to vegetation density and species composition, which are likely to drive understory presence and the type and amount of litter. However, fine-scale variation of surface fuel components is not adequately captured with these data; hence active remote sensing systems like drones equipped with LiDAR sensors, which are able to partly penetrate canopies and collect information about vertical forest structure and the forest floor,

may be useful in the direct mapping of laying trunks, shrubs or even the presence of herbs and grasses.

In scientific literature, different studies report the success of LiDAR data for estimating forest attributes (Bottalico et al., 2017, Zhao et al., 2011), quantify post-disturbance structural characteristics (Bolton et al., 2015, McCarley et al., 2017), fire severity assessment (García et al., 2020, Montealegre et al., 2014) and vegetation recovery analysis (Gordon et al., 2017, Martín-Alcón et al., 2015). The use of low-density LiDAR data has also proved its ability to estimate forest attributes in Mediterranean forests (Gelabert et al., 2020, Tijerín et al., 2022), providing a suitable representation of the post-fire forest conditions attending to both vertical structure and horizontal continuity of vegetation (Kane et al., 2010). Estimates of vegetation cover and height as well as structural heterogeneity provide valuable information on how the dominance of shrub and tree strata is shifting within the recovery process (Bartels et al., 2016). However, the fusion of LiDAR with multispectral data can provide both direct and indirect measurements of surface fuels and may thus lead to more accurate mapping both within and across different forest types. Studies combining ALS with multispectral information have found moderate improvements in predicting surface fuel load variation for different forest types (Bright et al., 2017; Stefanidou et al., 2020).

6.2.4. Multispectral and hyperspectral imaging

These techniques capture data across multiple wavelengths, beyond the visible spectrum. UAS equipped with multispectral or hyperspectral sensors capture images in different spectral bands, providing detailed information about the composition of surfaces. Multispectral and hyperspectral data are highly valuable for specific applications such as agriculture and environmental monitoring. These datasets can be integrated with other mapping techniques to provide comprehensive analysis but require specialized software for processing and analysis.

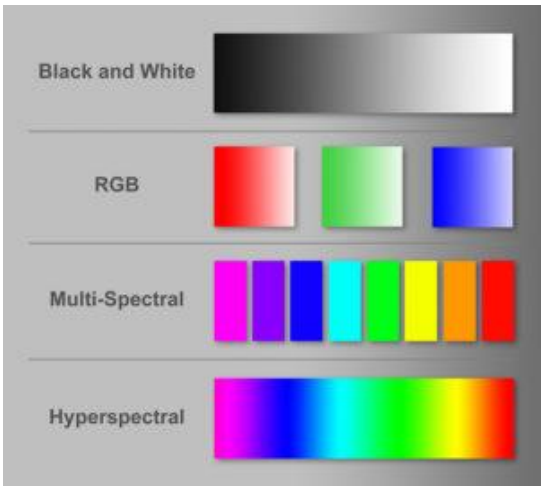

Figure 13. Different modes of imaging illustrating the benefits of hyperspectral imaging. (https://www.middletonspectral.com/resources/what-is-hyperspectral-imaging/)

For fire detection and monitoring, multispectral imaging is generally more suitable due to its efficiency in detecting heat and flames, faster processing times and lower data volume, and cost-effectiveness and ease of use.

Multi-wavelength techniques are useful for fire detection as well as for radiometric measurements. Sensor systems integrating several infrared bands are common for sophisticated fire detection and monitoring instruments used on satellites and high-altitude aircraft. For example, the autonomous modular sensor (AMS-Wildfire) can scan a broad path of ground from a UAV (Ambrosia et al., 2011) or pressurized inhabited aircraft Schroeder et al., 2014) (field of view selectable at 43° or 86° trading off with resolution) at 12 spectral bands from 0.42 to 11.26 μm (visible to thermal infrared VIS-TIR). Usually in the infrared regions four dual-gain bands are scanned at both a high gain and a low gain to allow a wide temperature measurement range. The spectral range and selectivity allow for multi-band detection algorithms (Ambrosia et al., 2014; Li et al., 2001), that compare pixel temperature in the MWIR with responses in TIR and Visible range to reduce false detections.

Nighttime imaging provides another opportunity to avoid the effects of reflected sunlight on MWIR (and SWIR) sensing. As thermal sensing aims to detect emitted rather than reflected energy it can be performed both day and night. A disadvantage of nighttime sensing is that wildfires tend to have a strong diurnal cycle and size and intensity of the fire often decreases markedly overnight (Hinkley et al., 2011).

6.2.5. Thermal Imaging

Thermal imaging detects heat emitted by objects, which is useful for identifying temperature variations. UAS equipped with thermal cameras capture thermal radiation, which is processed to create thermal maps. Thermal imaging data can be used in conjunction with other types of data (like RGB imagery and LiDAR) for applications such as energy audits and search and rescue. However, integration requires specialized software capable of handling thermal data.

Aerial photography or videography remains the most commonly performed tasks with drones. For this purpose, drones are equipped with one or multiple cameras, enabling them to capture their surroundings from the air.

In the field of cameras, there are two main types of sensors: standard camera sensors and thermal camera sensors. Standard camera sensors, also known as visible-light cameras or RGB cameras, capture images using the visible spectrum of light with red, green, and blue channels to create full-color images. These cameras are commonly used for regular photography and videography in typical lighting conditions. On the other hand, thermal camera sensors, also called infrared cameras, detect infrared radiation emitted by objects based on their temperature, allowing visualization of heat variations in a scene. Thermal cameras are valuable for applications like night vision, firefighting, search and rescue operations, industrial inspections, and identifying heat leaks in buildings. Utilizing IR cameras presents a favourable solution for fire detection and localization. The technique's advantages stem from its ability to identify highly luminous pixels against a dark background, enabling the distinction between fires and other objects, such as animals, through suitable algorithms. In scenarios where conventional RGB images encounter limitations due to dense vegetation and inherent variations in lighting within forest environments, thermal imaging emerges as a promising avenue for wildfire detection. By virtue of their capability to capture the distinctive heat emissions associated with combustion activities, thermal images transcend the constraints of traditional visual methods. By circumventing the visual impediments posed by dense foliage, thermal images enable a more accurate detection of fire hotspots, thereby facilitating early identification and swift response in managing emergency situations related to forest fires.

The thermal sensitivity of a thermal camera measures its ability to detect subtle temperature differences, thereby enabling visualization of objects with minimal thermal variations. These cameras can operate in different ranges of the infrared spectrum, typically categorized as near-infrared (NIR),

mid-infrared (MIR), and far-infrared (FIR), each having specific applications. However, thermal images may be influenced by weather conditions, absorption, and reflection of infrared radiation, as well as the distance between the object and the camera, which can impact their quality and accuracy.

However, there are certain drawbacks associated with this approach. One primary limitation is the inability to detect and classify clouds. Consequently, it becomes challenging to differentiate a cloud with a dense concentration of smoke, indicating a fire, from a typical hydrometeor. In this context, also for these reasons, the detection of fires in videos using both the visible and (IR) spectrum is a powerful approach that enhances the capabilities of fire detection systems. In fact, by analysing video footage captured in both spectra, advanced computer vision algorithms can effectively identify and alert authorities to the presence of fires in real-time. Video-based fire detection using the visible and IR spectrum leverages the distinct characteristics of flames, smoke, and heat emitted by fires. The visible spectrum captures the visual cues of flames and smoke, while the IR spectrum detects the thermal signatures and temperature anomalies associated with fire events.

6.2.6. Real-time data transfer and live video streaming

Real-time data transfer and live video streaming provide immediate insights during UAS operations. UAS transmits data and video feed to ground control stations in real-time, enabling live monitoring and quick decision-making. Real-time data transfer and video streaming are useful for immediate decision-making and surveillance. Integration with other data types can be challenging due to the need for robust communication links and real-time processing capabilities.

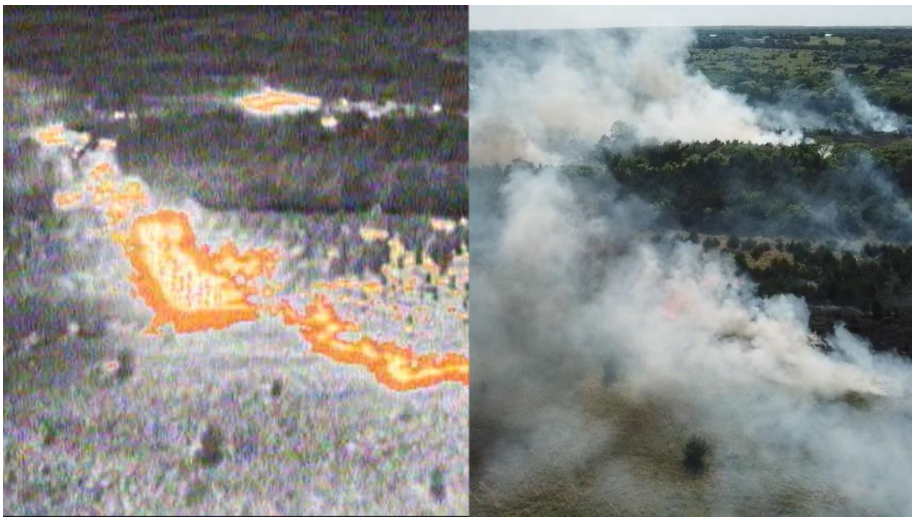

Figure 14. The fire event viewed with two different cameras, conventional RGB (right) and infrared (left); Source: (https://extension.okstate.edu/fact-sheets/using-drones-with-infrared-capabilities-to-monitor-fire-behavior.html)

6.2.7. Geometrical evaluation

This involves analyzing the geometrical properties of the surveyed area to ensure accuracy. Data collected by UAS is processed to evaluate geometric accuracy, such as distances, angles, and volumes. Geometrical evaluation data is essential for ensuring the accuracy of survey data. This data can be integrated into most surveying and mapping software, enhancing the precision of the final outputs.

6.2.8. Aerial Action

Aerial actions utilise techniques to enhance operational effectiveness regarding particular application. Among aerial action techniques, sound diffusion and lighting can be distinguished as most effective.

6.2.9. Sound diffusion technique

This technique implies that the drone is equipped with loudspeaker/s, in order that emits sound across a specific area. The sound is generated as an audible alert or information, depending on a particular situation.

Examples of sound messages can be information about the flight, specific actions, public announcements (PA), crowd control, various types of orders, etc. One of the main features of this technique is the insurance of even sound distribution over the large or difficult to access area. Sound diffusion technique is valuable in environments where usual, fixed PA systems are not feasible (e.g. forests).

Table 4. UAS sound diffusion geographical features.

Height Range	Use Case	Benefits	Limitations	Feasible Areas
Low Altitudes				
0-100 meters	- Localized sound diffusion	- Clearer sound transmission	- Limited area coverage	- Small-scale areas (under 1 km²)
	- Crowd management or public announcements	- Less sound loss	- May not be suitable for densely populated areas	- Construction sites, rallies
	- Wildlife deterrence		- Noise interference at ground level	
Medium Altitudes				
100-300 meters	- Medium-sized area sound diffusion	- Moderate area coverage	- Some sound attenuation	- Medium-scale areas (1-5 km²)
	- Wildlife management or search/rescue	- Suitable for parks, wildlife areas	- Requires moderate sound power	- Parks, agriculture, search & rescue
High Altitudes				
300 meters and above	- Large-scale sound diffusion	- Wider area coverage	- Significant sound attenuation at higher altitudes	- Large-scale areas (5-10 km²)
	- Emergency response, military use	- Can cover vast regions	- Requires high-powered emitters	- Disaster zones, military operations
			- Drone regulations may limit operations	
Feasibility Factors	- Weather conditions (wind, humidity)	- Clear conditions improve sound quality	- Poor weather can degrade sound performance	
	- Airspace regulations	- Safe, regulated drone operations	- Restricted operations in populated areas	
	- Drone battery life & payload capacity	- Drones can operate longer with efficient power	- Payload limits may restrict sound system size	

Generally, the effective height for a power of approximately 100 dB is 30 meters. The effective heights, areas, and feasibility considerations for sound diffusion using UASs is presented in Table 4.

6.2.10. Lighting technique

Areas difficult to access can be investigated and approached with UAS equipped with spotlights, i.e. powerful lighting systems. The application of lighting technique is reflected in search and rescue operations, surveillance, disaster response, inspection, etc. This technique enables operators to illuminate large areas from above, significantly enhancing visibility in low-light or night-time environments. The usage of LED or other high-intensity light sources enables the provision of focused lighting on demand.

The height at which lighting UASs operate depends on the power of the light source and the area that needs to be illuminated. Typical operational altitudes for lighting drones range from 50 to 150 meters, though this may vary depending on the specific scenario (Table 5).

Table 5. UAS lighting geographical and effective features.

Height Range (meters)	Area of Illumination (square meters)	Typical Application
0-50	500-1000	Close-range inspections, small search areas
50-100	1000-5000	Larger rescue operations, moderate area surveillance
100-150	5000-10000	Large-area disaster response, mass casualty management

In order to achieve optimal results, one of the main features of UAS lighting technique is the illumination angle, or *beam spread*. It is the angular dispersion of light emitted from the drone's lighting system. It determines how wide or narrow the light will spread as it travels from the source (UAS) to the target area. The angle of the light relative to the ground changes with the altitude of the drone, affecting the size of the illuminated area. The key features of angles in UAS lighting techniques are presented in Table 6.

Table 6. UAS aerial action lighting technique: key features

Aspect	Feature	Details	Application
Illumination Angle	Narrow Beam (10-30 degrees)	Focused lighting with high intensity. Useful for precision tasks, e.g., infrastructure inspection.	**Power line inspection**, **building inspection**, **search and rescue in confined spaces**.
	Wide Beam (40-120 degrees)	Broad lighting with lower intensity. Covers large areas but with less focus.	**Search and rescue** in open areas, **disaster relief**, **general surveillance** of large areas.
Altitude vs. Coverage	Low Altitude (0-50 meters)	Narrow beams cover small areas with high intensity. Wide beams offer clear lighting for confined areas.	**Close-up inspections**, **patrolling**, **security in confined areas**.
	Medium Altitude (50-100 meters)	Moderate coverage with narrow beams and broader coverage with wide beams.	**Search and rescue missions**, **surveillance over moderate areas**, **firefighting operations**.
	High Altitude (100-150 meters)	Extensive area coverage with wide beams but with reduced intensity. Narrow beams provide focused lighting at greater distances.	**General surveillance** over large open areas, **long-distance identification** of targets.
Angle of Incidence	Direct Incidence (90 degrees)	Maximum light efficiency, uniform illumination across the surface, no shadowing.	**Road inspections**, **flat terrain illumination**, **open area surveillance**.
	Oblique Incidence (< 90 degrees)	Reduced efficiency with elongated shadows. Enhances contrast for object detection in specific scenarios.	**Surface anomaly detection**, **shadow-based observation**, **rugged terrain inspections**.
Adjustable Lighting	Gimbal/Tilting Systems	Real-time control of lighting angles, compensating for drone movement or varying terrain.	**Dynamic search and rescue** missions, **real-time target tracking** in security operations, **inspections requiring frequent lighting adjustments**.

Field of View (FOV)	Wide FOV with Matching Wide Beam	Ensures the entire scene captured by the camera is properly illuminated.	Surveillance, disaster recovery, search missions over broad areas.
	Narrow FOV with Matching Narrow Beam	Focuses on small, specific zones, with intense illumination for detailed observation.	**Infrastructure inspection**, **targeted security observations**, **precision search in rescue operations**.

6.3. Mapping approaches

6.3.1. Rectangle mapping

Rectangle mapping Involves flying in a rectangular grid pattern to cover the survey area comprehensively. The grid-based approach of rectangle mapping is compatible with most surveying and mapping software. It ensures comprehensive coverage and is easy to process with standard tools.

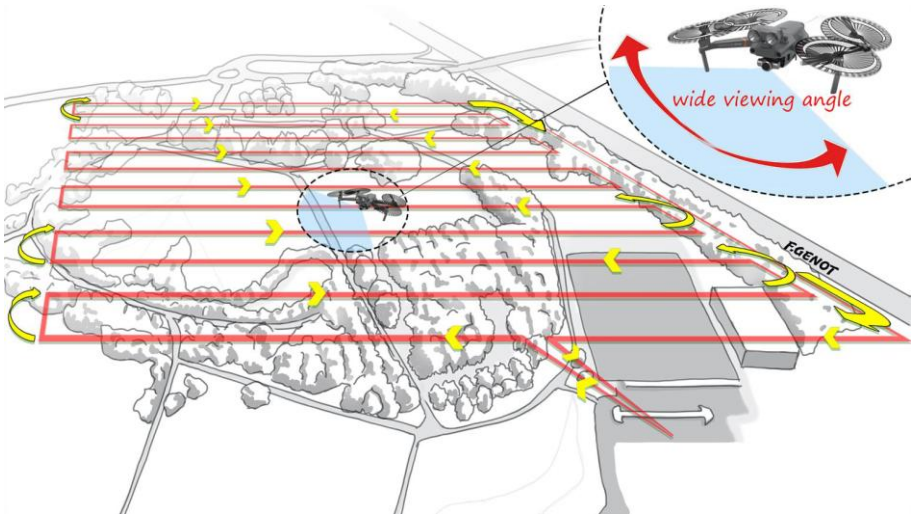

Figure 15. UAS rectangle mapping data collection technique.

The mapping technique consists of programming a zone rollover plan mapping, automatic flight as pilot monitoring to capture images, recovery of captured images, treatment of images in photogrammetry software, and the production of a 2-dimensional orthophoto mosaic map.

6.3.2. Spiral mapping

This technique is used for detailed surveys of specific areas by flying in a spiral pattern from a central point. Spiral mapping is useful for focused areas and can be integrated with other mapping data. However, it might require specialized processing techniques to handle the unique flight pattern.

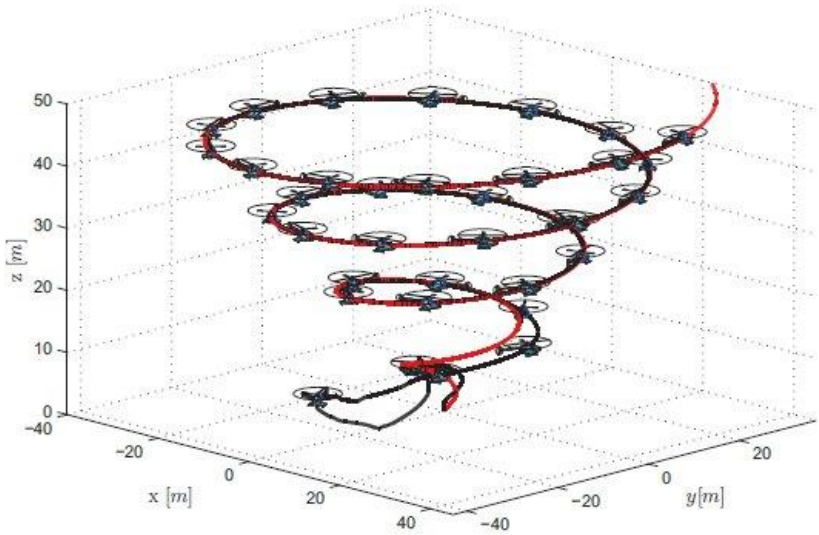

Figure 16. UAS spiral path (source: https://doi.org/10.5755/j01.itc.45.1.12413)

The spiral technique breaks down as follows; i) a circular evolution around the building to collect 4 photos (ABCD facades); ii) a circular evolution to capture a short video of the 4 facades of the building; iii) a vertical shift centered to capture a photo of the roof (R) and the tactical situation as a whole (Figure 16).

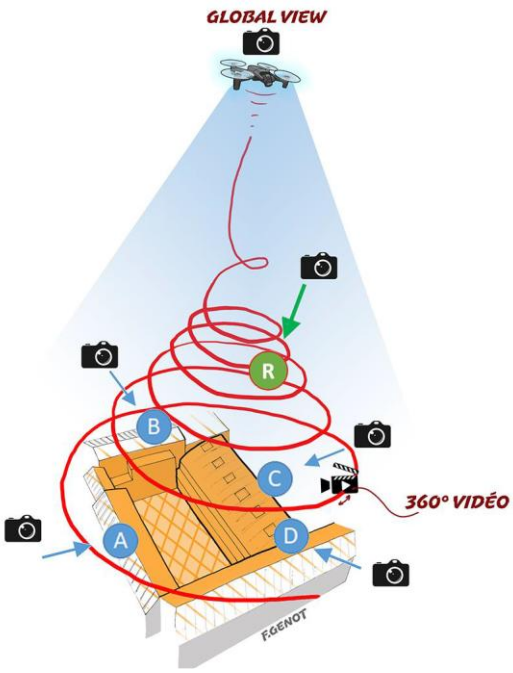

Figure 17. UAS spiral technique.

6.4. Interoperability

Interoperability in UAS data collection techniques refers to the ability of different systems and methods to work together seamlessly. The

interoperability of UAS data collection techniques largely depends on the standardization of data formats and the compatibility of processing software. Techniques like 2D/3D photogrammetry, ortho-mosaic mapping, and LiDAR are highly interoperable due to their widespread use and standardized outputs. Multispectral/hyperspectral imaging and thermal imaging, while highly valuable, require specialized software for full integration. Real-time data transfer and video streaming offer immediate insights but need robust systems for real-time processing. The interoperability matrix between data collection techniques is presented in Table 7.

Table 7. Interoperability matrix.

		P	OM	L	MHI	TI	R	GE	M	
									R	S
P		-	H	H	M	M	M	H	H	M
OM		H	-	H	M	M	M	H	H	M
L		H	H	-	M	M	M	H	H	M
MHI		M	M	M	-	M	M	M	M	M
TI		M	M	M	M	-	M	M	M	M
R		M	M	M	M	M	-	M	M	M
GE		H	H	H	M	M	M	-	H	M
M	**R**	H	H	H	M	M	M	H	-	M
	S	M	M	M	M	M	M	M	M	-

M *– medium interoperability;* ***H*** *– high interoperability;* ***P*** *– 2D/3D Photogrammetry;* ***OM*** *– Ortho-mosaic Mapping;* ***MHI*** *– Multispectral/Hyperspectral Imaging;* ***L*** *– LiDAR;* ***TI*** *– Thermal imaging;* ***R*** *– Real-time Data Transfer & Live Video Streaming,* ***GE*** *- Geometrical Evaluation;* ***R*** *– Rectangle Mapping;* ***S*** *– Spiral Mapping*

The Figure 17 shows most common UAS aerial surveying and mapping techniques, and levels of interoperability.

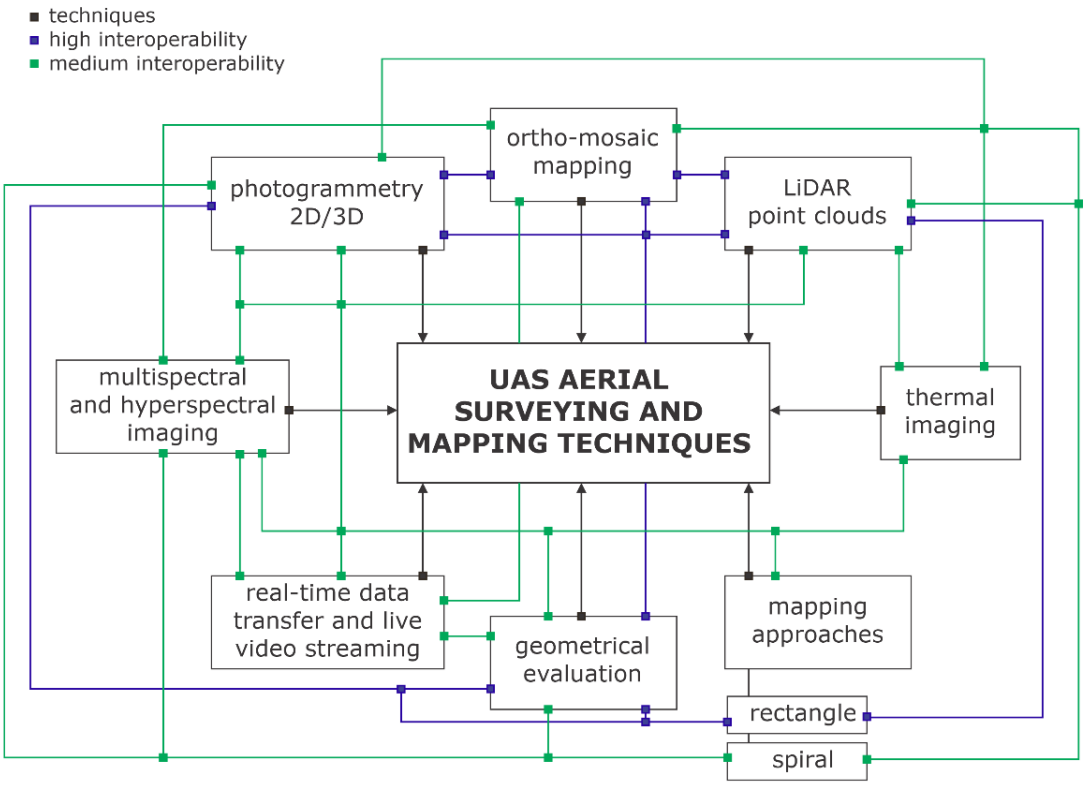

Figure 18. UAS aerial surveying and mapping techniques, and levels of interoperability

The extended information on data collection methods, their description, interoperability, importance and quality are presented in Table 8.

Table 8. Description and interoperability between data collection techniques.

Technique	Description	Interoperable with	Importance[1]	Quality[2]
2D/3D Photogrammetry	Captures images from different angles to create 2D maps and 3D models	Ortho-Mosaic Mapping, Point Clouds, Thermal Imaging	High	High
Ortho-Mosaic Mapping	Generates geometrically corrected maps with uniform scale	2D/3D Photogrammetry, Thermal Imaging	High	Very High

[1] The **importance** parameter reflects the criticality of the technique in various application; *medium* – techniques that are essential for certain specialized tasks but not universally critical, *high* – techniques widely used in various applications, providing essential data, v*ery high* - techniques that are crucial across many applications, providing foundational data for multiple analyses.
[2] The **quality** parameter assesses the accuracy and reliability of data provided by each technique; high – provides accurate and reliable data for most applications, very high – offers superior accuracy and reliability, often forming the backbone of detailed analysis.

Point Clouds	Dense collection of points representing 3D structures, captured using LIDAR or photogrammetry	2D/3D Photogrammetry, Thermal Imaging	Very High	Very High
Thermal Imaging	Captures temperature variations, identifying heat sources or anomalies	2D/3D Photogrammetry, Ortho-Mosaic Mapping, Point Clouds	High	High
Multispectral Imaging	Captures data across multiple light wavelengths, beyond the human eye	Hyperspectral Imaging, 2D/3D Photogrammetry	Medium	High
Hyperspectral Imaging	Captures comprehensive spectral data across a wide range of wavelengths	Multispectral Imaging, 2D/3D Photogrammetry	Medium	Very High
Real-time Data Transfer and Live Video Streaming	Sending data and video feed in real-time	Thermal imaging, multispectral imaging	High	High
Geometrical evaluation	Analyzing geometric properties for precise measurements	3D photogrammetry, LiDAR	High	High
Rectangle Mapping	Covering areas in a systematic rectangular pattern	Ortho-mosaic mapping	Medium	Medium
Spiral Mapping	Covering areas in a spiral pattern for detailed central focus	Ortho-mosaic mapping	Medium	Medium

Most techniques exhibit medium to high interoperability, particularly when used in conjunction with standard formats and comprehensive processing software. Integration is most seamless between methods like 2D/3D Photogrammetry, Ortho-Mosaic Mapping, and LiDAR, while spectral and thermal imaging require more advanced data fusion techniques.

6.5. Scope of application/Mission actions/mode of operation:

6.5.1. General considerations and an overview in data collection techniques' applications

The UAS with their remote sensing techniques enable a variety of applications ranging in their nature. The applications can be roughly and broadly categorised as ***i)*** agricultural and environmental applications, ***ii)*** intelligence, surveillance, and reconnaissance, ***iii)*** aerial monitoring in engineering, ***iv)*** cultural heritage, and ***v)*** traditional surveying, conventional mapping and photogrammetry, and cadastral applications.

As for employed data collection techniques, the application examples are presented in Table 9.

Table 9. Examples of particular UAS data collection techniques' applications

Technique		**Application examples**
Photogrammetry	**2D**	Urban planning, agriculture, land use mapping, topographic mapping, and environmental monitoring
	3D	Construction site monitoring, historical site documentation, and infrastructure inspection
Ortho-Mosaic Mapping		Agriculture (e.g. crop health monitoring), forestry (e.g. tree count and health), land surveying, environmental studies, disaster management
LiDAR (point clouds)		Topographic mapping, forestry (e.g. canopy height measurement), flood risk assessment, heritage conservation
Multispectral and Hyperspectral Imaging		Precision agriculture/ advanced agricultural analysis (e.g. crop health assessment), environmental monitoring (e.g. pollution detection), mineral exploration, fire assessment (e.g. thermal anomalies' detection, burned and unburned vegetation differentiation, post-fire recovery monitoring)
Thermal Imaging		Energy audits (e.g. detecting heat leaks in buildings), search and rescue operations (locating missing persons), wildlife monitoring, firefighting, fire detection
Real-time Data Transfer and Live Video Streaming		Surveillance, disaster response, and military operations
Geometrical Evaluation		Engineering, construction, and scientific research

Mapping	**Rectangle**	Large area surveys like agriculture fields or urban planning
	Spiral	Disaster site surveys, archaeological sites

Different applications in terms of remote sensing are shown in Figure 18.

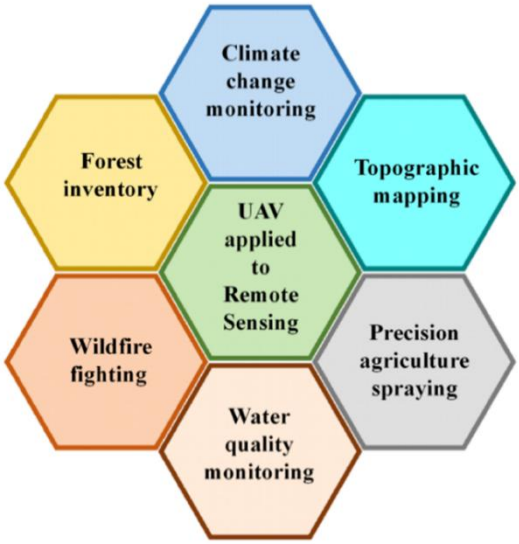

Figure 19. UAS aerial surveying and mapping techniques, and levels of interoperability (10.3390/drones6060147).

6.5.2. Mission actions' application examples

The UAS have become pivotal in enhancing various mission actions across different operational scopes. Their advanced technologies and versatile applications allow for real-time visual observation, thermal imaging, firefighting support, search and rescue operations, and post-event investigation and analysis.

Search for danger: In emergency situations, UAS can be deployed to search for potential dangers, such as hazardous materials, structural damage, or trapped individuals. Their ability to access hard-to-reach areas makes them invaluable for disaster response and management.

UAS provide ***security and technical escort*** services by monitoring and protecting assets, personnel, and infrastructure. They can patrol perimeter fences, monitor crowds, and provide aerial support during transport of high-value items or sensitive operations.

Real-Time Visual Observation, in terms of *Safety Watch* and *Patrol Mode* refers to continuous monitoring of areas for security purposes, inspecting infrastructure, as well as environmental monitoring and surveillance.

Detection of Hot Spots in function of early warnings aims at identifying potential fire hazards or equipment overheating. Depending on several data collection and monitoring techniques and technologies thermal imaging is presented: on the example of detecting hot spots in a forest to provide early warnings for wildfire prevention.

Table 10. Steps in Hot Spot Detection with Multiple Techniques.

Step	Description
Planning	Define objectives, plan flight paths, and check equipment
Deployment	Launch UAS, navigate using GPS, capture data using thermal, multispectral, hyperspectral, and visual/IR sensors
Data Collection	Monitor data feed, ensure stable flight for high-quality data
Analysis	Process images, identify hot spots, georeference data
Reporting	Generate alerts, communicate findings to authorities, provide coordinates and temperature/spectral data
Follow-Up	Conduct additional flights to monitor hot spots and verify mitigation measures

Logistic Support for Search and Rescue and Search and Recovery operations in locating missing persons, delivering supplies, and providing situational awareness (especially in remote areas).

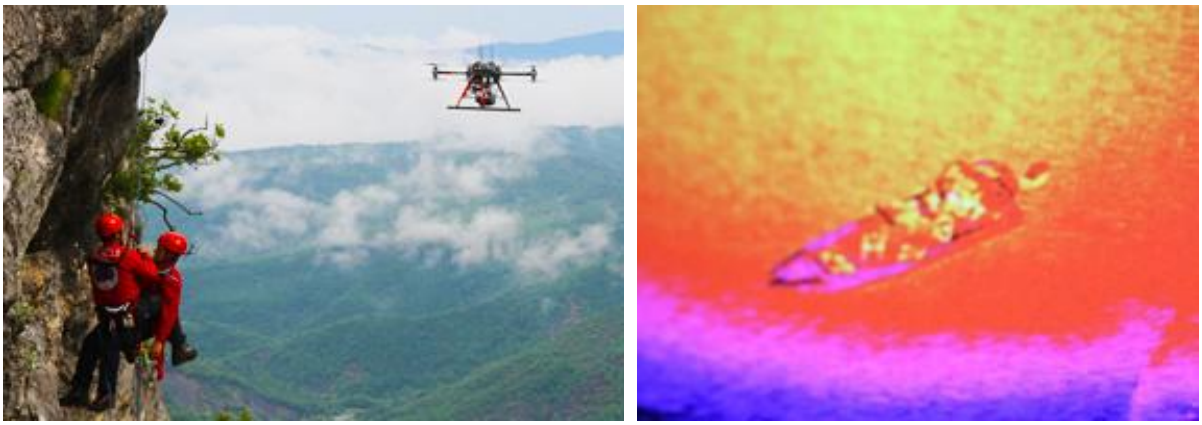

Figure 20. Drone support for Search and Rescue Operations (https://altigator.com/en/drones-for-search-rescue-missions/)

Post-Event Investigation and analysis – Recording/Mass Casualty: Documenting the aftermath of natural disasters or accidents for analysis and reconstruction (e.g. creation of detailed maps of areas affected by a flood/fire/other in order to assess damage, impacts, plan recovery efforts.... aim: to improve future response strategies.

From real-time visual observation and thermal imaging to firefighting support and SAR operations, UAS enhance the effectiveness and efficiency of various missions. Their role in post-event investigation and analysis further underscores their value in modern operational strategies.

Drone forensics is a specialized field of digital forensics focused on the collection, analysis, and interpretation of UAS data. Their use in criminal activities, accidents, and security breaches is growing, necessitating robust forensic methodologies to extract and analyse data from these devices. Key aspects of drone forensics are Data collection from drones, Types of data, Forensic methodology, Legal and ethical considerations, and Application of forensics.

Support for Firefighting Operations, providing real-time data and thermal imaging to support ground firefighting teams (e.g. mapping the extent of a fire and identifying the hottest areas to prioritize firefighting efforts). In general, the integration of advanced sensors and communication systems makes UASs an invaluable asset in managing and mitigating fire-related incidents. They enhance firefighting capabilities by providing critical, real-time information, improving safety for human responders, and enabling more efficient and effective resource deployment. Their ability to gather data in hazardous and hard-to-reach areas, coupled with advanced imaging and mapping technologies, makes them indispensable in modern fire management strategies.

Key applications of UASs in firefighting consist of more previously described mission actions and data collection techniques and can be categorised as follows: ***i)*** Real-time aerial observation; ***ii)*** Thermal imaging for hotspot detection; ***iii)*** Geospatial mapping and 3D modelling; ***iv)*** Communications relay and coordination; ***v)*** Logistics support; and ***vi)*** Post event analysis and documentation.

6.5.3. Operational capacity of the FRED platform – data transmission and viewing optimisation

The preferred minimum computing power for the best resolution (1440p-4K) of the FRED platform user stations is specified as follows:

Processor: Intel Core i7 (10th gen or newer) or equivalent

RAM: 16 GB or more

Graphics: Dedicated graphics card with 8 GB VRAM (NVIDIA GeForce GTX 1660, RTX 2060 or equivalent)

Storage: 512 GB SSD or larger

Internet Speed: 50 Mbps or higher

Monitor: 27" screen with 2560x1440 resolution or better

7. Concluding remarks

Developed collaboratively by a multi-national consortium, this methodology combines advanced geospatial technologies, remote sensing, UAV applications and weather data to build a harmonized cross-border approach to wildfire risk management.

The report outlines a multi-layered strategy that integrates land cover analysis, fuel mapping, fire behaviour modelling and meteorological forecasting. Key innovations include the use of Object-Based Image Analysis (OBIA) for high-resolution fuel classification, the deployment of sophisticated UAV platforms equipped with RGB, thermal, LiDAR, and multispectral sensors, and the application of FlamMap and Fire Danger Index (FDI) modelling for dynamic risk assessment. Additionally, the integration of real-time weather data from the MISTRAL platform ensures accurate fire weather forecasting capabilities.

This methodology not only advances technical capabilities in data collection and analysis but also fosters interoperability among tools and institutions across partner countries. Having based this methodology on scientific groundwork and operational feasibility, the project strengthens regional resilience against wildfires while supporting EU climate adaptation and disaster risk reduction objectives.

In conclusion, the Fire Free MED methodology establishes a strong foundation for informed decision-making, transnational collaboration and future policy development, offering a replicable model for other fire-prone regions in Europe and beyond.

Appendix A:

Template for Use Case specification and scenario setup

Note: To support practical implementation, the appendix provides a structured template for specifying use cases and setting up scenarios. This ensures that mission actions, techniques, and operational fields are clearly defined and aligned with the data collection capabilities.

USE CASE No. 1*

Title:	
Description:	

FIELD / SCOPE OF ACTION	*Check*
Prevention and mitigation	☐
Active emergency response /S&R	☐
Post-fire status damage assessment	☐

MISSION ACTION	*Check*
Real-time visual observation	☐
Hot spot detection	☐
Search for danger	☐
Security and technical escort	☐
Logistic support	☐
Support in firefighting operations	☐
Post-event investigation and analysis	☐
Data collection	☐
*Other***	☐

TECHNIQUES	*Check*
Real-time Data Transfer	☐
Thermal Imaging	☐
Live Video Streaming	☐
Geometrical evaluation (range, bearing, POI)	☐
Rectangle and Spiral Mapping	☐
Sound diffusion	☐
Lighting	☐
Multispectral Imaging	☐
Ortho-Mosaic Mapping	☐
Photogrammetry	☐
LiDAR - point clouds	☐
Other**	☐

**For each Use case, the dependency between actions, missions and techniques must be satisfied.*
*** Specify only if none of the existing ones suit the requirements.*

Appendix B:

Flight logging form in the FRED platform

Note: To ensure accurate operational tracking and accountability, the appendix presents the standard flight logging form used within the FRED platform. This form combines automated flight metrics with manual input of team and mission details for comprehensive record-keeping.

FLIGHT LOG*

	Start	**End**	**Duration**	**Location**
Flight log	*(auto fill)*	*(auto fill)*	*(auto fill)*	*(Link to map)*

	Team member name (first, last, *free text*)	**Role** (select single/ multiple), *dropdown menu*)
Flight team		

	Use case (select *dropdown menu*, predefined - from this document)	**Note**
Operation		

*****Flight logging will be done through a form in the FRED application. The data in the log on flight metrics will be filled in automatically (start/end/duration/location), whereas a staff member will insert Flight team data (roles and their holders). After inputting staff member name, corresponding role(s) will be selected from a drop-down menu.

References

1. Ambrosia, V. G., Wegener, S., Zajkowski, T., Sullivan, D. V., Buechel, S., Enomoto, F., Lobitz, B., Johan, S., Brass, J., & Hinkley, E. (2011). The Ikhana unmanned airborne system (UAS) western states fire imaging missions: From concept to reality (2006–2010). *Geocarto International*, 26, 85–101.
2. Bartels, S. F., Chen, H. Y. H., Wulder, M. A., & White, J. C. (2016). Trends in post-disturbance recovery rates of Canada's forests following wildfire and harvest. *Forest Ecology and Management*, 361, 194–207. https://doi.org/10.1016/j.foreco.2015.11.015
3. Bock, M., Xofis, P., Rossner, G., Wissen, M., & Mitchley, J. (2005). Object oriented methods for habitat mapping in multiple scales: Case studies from Northern Germany and North Downs, GB. *Journal for Nature Conservation*, 13(2–3), 75–89.
4. Bolton, D. K., Coops, N. C., & Wulder, M. A. (2015). Characterizing residual structure and forest recovery following high-severity fire in the western boreal of Canada using Landsat time-series and airborne lidar data. *Remote Sensing of Environment*, 163, 48–60. https://doi.org/10.1016/j.rse.2015.03.004
5. Bottalico, F., Chirici, G., Giannini, R., Mele, S., Mura, M., Puxeddu, M., McRoberts, R. E., Valbuena, R., & Travaglini, D. (2017). Modeling Mediterranean forest structure using airborne laser scanning data. *International Journal of Applied Earth Observation and Geoinformation*, 57, 145–153. https://doi.org/10.1016/j.jag.2016.12.013
6. Bright, B. C., Hudak, A. T., Kennedy, R. E., Braaten, J. D., & Henareh Khalyani, A. (2019). Examining post-fire vegetation recovery with Landsat time series analysis in three western North American forest types. *Fire Ecology*, 15, 2. https://doi.org/10.1186/s42408-018-0021-9
7. Calkin, D. E., Ager, A. A., & Gilbertson-Day, J. (2010). Wildfire risk and hazard: Procedures for the first approximation (Gen. Tech. Rep. RMRS-GTR-235). U.S. Department of Agriculture, Forest Service, Rocky Mountain Research Station.
8. Catry, F. X., Rego, F. C., Bacao, F., & Moreira, F. (2009). Modelling and mapping wildfire ignition risk in Portugal. *International Journal of Wildland Fire*, 18, 921–931.
9. Colomina, I., & Molina, P. (2014). Unmanned aerial systems for photogrammetry and remote sensing: A review. *ISPRS Journal of Photogrammetry and Remote Sensing*, 92, 79–97.
10. Drusch, M., et al. (2012). Sentinel-2: ESA's optical high-resolution mission for GMES operational services. *Remote Sensing of Environment*, 120, 25–36.
11. Federal Aviation Administration. (2020). *Advisory Circular 107-2, Small Unmanned Aircraft Systems (sUAS)*. FAA. https://www.faa.gov
12. Founda, D., & Giannakopoulos, C. (2009). The exceptionally hot summer of 2007 in Athens, Greece—a typical summer in the future climate? *Global and Planetary Change*, 67, 227–236.
13. García, M., North, P., Viana-Soto, A., Stavros, N. E., Rosette, J., Martín, M. P., Franquesa, M., González-Cascón, R., Riaño, D., Becerra, J., & Zhao, K. (2020). Evaluating the potential of LiDAR data for fire damage assessment: A radiative transfer model approach. *Remote Sensing of Environment*, 247, Article 111893. https://doi.org/10.1016/j.rse.2020.111893

14. Gelabert, P. J., Montealegre, A. L., Lamelas, M. T., & Domingo, D. (2020). Forest structural diversity characterization in Mediterranean landscapes affected by fires using Airborne Laser Scanning data. *GIScience & Remote Sensing*, 57, 497–509. https://doi.org/10.1080/15481603.2020.1738060
15. Gordon, C. E., Price, O. F., & Tasker, E. M. (2017). Mapping and exploring variation in post-fire vegetation recovery following mixed severity wildfire using airborne LiDAR. *Ecological Applications*, 27, 1618–1632. https://doi.org/10.1002/eap.1555
16. Hinkley, E. A., & Zajkowski, T. (2011). USDA Forest Service–NASA: Unmanned aerial systems demonstrations—Pushing the leading edge in fire mapping. *Geocarto International*, 26, 103–111.
17. International Emergency Drone Organization. (2022). *International report on best practices in robotics*. IEDO.
18. Kane, V. R., McGaughey, R. J., Bakker, J. D., Gersonde, R. F., Lutz, J. A., & Franklin, J. F. (2010). Comparisons between field- and LiDAR-based measures of stand structural complexity. *Canadian Journal of Forest Research*, 40, 761–773. https://doi.org/10.1139/X10-024
19. Kim, M., Madden, M., & Warner, T. (2009). Forest type mapping using object-specific texture measures from multispectral Ikonos imagery: Segmentation quality and image classification issues. *Photogrammetric Engineering & Remote Sensing*, 75, 819–829.
20. Li, Z., Kaufman, Y. J., Ichoku, C., Fraser, R., Trishchenko, A., Giglio, L., Jin, J. Z., & Yu, X. A. (2001). Review of AVHRR-based active fire detection algorithms: Principles, limitations, and recommendations. In F. J. Ahern, J. G. Goldammer, & C. O. Justice (Eds.), *Global and Regional Vegetation Fire Monitoring from Space, Planning and Coordinated International Effort* (pp. 199–225). Kugler Publications.
21. Martín-Alcón, S., Coll, L., De Cáceres, M., Guitart, L., Cabré, M., Just, A., & González-Olabarría, J. R. (2015). Combining aerial LiDAR and multispectral imagery to assess postfire regeneration types in a Mediterranean forest. *Canadian Journal of Forest Research*, 45, 856–866. https://doi.org/10.1139/cjfr-2014-0430
22. McCarley, T. R., Kolden, C. A., Vaillant, N. M., Hudak, A. T., Smith, A. M. S., Wing, B. M., Kellogg, B. S., & Kreitler, J. (2017). Multi-temporal LiDAR and Landsat quantification of fire-induced changes to forest structure. *Remote Sensing of Environment*, 191, 419–432. https://doi.org/10.1016/j.rse.2016.12.022
23. Montealegre, A. L., Lamelas, M. T., Tanase, M. A., & De la Riva, J. (2014). Forest fire severity assessment using ALS data in a Mediterranean environment. *Remote Sensing*, 6, 4240–4265. https://doi.org/10.3390/rs6054240
24. New America Foundation. (2015). *Drones and aerial observation: New technologies for property rights, human rights, and global development*. New America Foundation. https://www.newamerica.org
25. Ricotta, C., Bajocco, S., Guglietta, D., & Conedera, M. (2018). Assessing the influence of roads on fire ignition: Does land cover matter? *Fire*, 1, 24.
26. Rittl, T., Cooper, M., Heck, R. J., & Ballester, M. V. R. (2013). Object-based method outperforms per-pixel method for land cover classification in a protected area of the Brazilian Atlantic rainforest region. *Pedosphere*, 23, 290–297.
27. Schroeder, W., Ellicott, E., Ichoku, C., Ellison, L., Dickinson, M. B., Ottmar, R. D., Clements, C., Hall, D., Ambrosia, V., & Kremens, R. (2014). Integrated active fire

retrievals and biomass burning emissions using complementary near-coincident ground, airborne and spaceborne sensor data. *Remote Sensing of Environment*, 140, 719–730.

28. Stefanidou, A., Gitas, Z., Korhonen, I., Stavrakoudis, L., Georgopoulos, D., & Erratum, N. (2020). LiDAR-based estimates of canopy base height for a dense uneven-aged structured forest. *Remote Sensing*, 12(19), 3116. https://doi.org/10.3390/rs12193116
29. Tijerín, J., Moreno-Fernandez, D., Zavala, M. A., Astigarraga, J., & García, M. (2022). Identifying forest structural types along an aridity gradient in peninsular Spain: Integrating low-density LiDAR, forest inventory, and aridity index. *Remote Sensing*, 14, 235. https://doi.org/10.3390/rs14010235
30. Tolika, K., Maheras, P., & Tegoulias, I. (2009). Extreme temperatures in Greece during 2007: Could this be a "return to the future"? *Geophysical Research Letters*, 36, L10813.
31. Xofis, P., Konstantinidis, P., Papadopoulos, I., & Tsiourlis, G. (2020). Integrating remote sensing methods and fire simulation models to estimate fire hazard in a south-east Mediterranean protected area. *Fire*, 3(3), 31. https://doi.org/10.3390/fire3030031
32. Xofis, P., Tsiourlis, G., & Konstantinidis, P. (2020). A fire danger index for the early detection of areas vulnerable to wildfires in the Eastern Mediterranean region. *Euro-Mediterranean Journal for Environmental Integration*, 5, Article 38.
33. Zhao, K., Popescu, S., Meng, X., Pang, Y., & Agca, M. (2011). Characterizing forest canopy structure with lidar composite metrics and machine learning. *Remote Sensing of Environment*, 115, 1978–1996. https://doi.org/10.1016/j.rse.2011.04.001